EBioMedicine 33 (2018) 169–184

Contents lists available at ScienceDirect

EBioMedicine

journal homepage: www.ebiomedicine.com

Research Paper

Initial Identification of a Blood-Based Chromosome Conformation Signature for Aiding in the Diagnosis of Amyotrophic Lateral Sclerosis

Matthew Salter [a], Emily Corfield [a], Aroul Ramadass [a], Francis Grand [a], Jayne Green [a], Jurjen Westra [a], Chun Ren Lim [a], Lucy Farrimond [b], Emily Feneberg [b], Jakub Scaber [b], Alexander Thompson [b], Lynn Ossher [b], Martin Turner [b], Kevin Talbot [b], Merit Cudkowicz [c], James Berry [c], Ewan Hunter [a], Alexandre Akoulitchev [a,*]

[a] Oxford BioDynamics, Oxford, UK
[b] Nuffield Department of Clinical Neurosciences, University of Oxford, John Radcliffe Hospital, Oxford OX3 9DU, UK
[c] Neurology Clinical Research Institute, Department of Neurology, Massachusetts General Hospital, Harvard Medical School, Boston, MA, United States

ARTICLE INFO

Article history:
Received 3 May 2018
Received in revised form 11 June 2018
Accepted 12 June 2018
Available online 23 June 2018

ABSTRACT

Background: The identification of blood-based biomarkers specific to the diagnosis of amyotrophic lateral sclerosis (ALS) is an active field of academic and clinical research. While inheritance studies have advanced the field, a majority of patients do not have a known genetic link to the disease, making direct sequence-based genetic testing for ALS difficult. The ability to detect biofluid-based epigenetic changes in ALS would expand the relevance of using genomic information for disease diagnosis.
Methods: Assessing differences in chromosomal conformations (i.e. how they are positioned in 3-dimensions) represents one approach for assessing epigenetic changes. In this study, we used an industrial platform, *EpiSwitch*™, to compare the genomic architecture of healthy and diseased patient samples (blood and tissue) to discover a chromosomal conformation signature (CCS) with diagnostic potential in ALS. A three-step biomarker selection process yielded a distinct CCS for ALS, comprised of conformation changes in eight genomic loci and detectable in blood.
Findings: We applied the ALS CCS to determine a diagnosis for 74 unblinded patient samples and subsequently conducted a blinded diagnostic study of 16 samples. Sensitivity and specificity for ALS detection in the 74 unblinded patient samples were 83·33% (CI 51·59 to 97·91%) and 76·92% (46·19 to 94·96%), respectively. In the blinded cohort, sensitivity reached 87·50% (CI 47·35 to 99·68%) and specificity was 75·0% (34·91 to 96·81%).
Interpretations: The sensitivity and specificity values achieved using the ALS CCS identified and validated in this study provide an indication that the detection of chromosome conformation signatures is a promising approach to disease diagnosis and can potentially augment current strategies for diagnosing ALS.
Fund: This research was funded by Oxford BioDynamics and Innovate UK. Work in the Oxford MND Care and Research Centre is supported by grants from the Motor Neurone Disease Association and the Medical Research Council. Additional support was provided by the Northeast ALS Consortium (NEALS).

1. Introduction

ALS is a fatal, degenerative neurologic disorder characterized by progressive muscle weakness and eventual paralysis. Disease presentation and rate of progression vary from patient-to-patient and while there are clinical tools to monitor disease progression after diagnosis (e.g. ALSFRS-R, FVC measures), no definitive clinically validated measure currently exists to diagnose the disease. Combined with the insidious nature of symptom onset, lack of recognition of symptoms and signs in non-specialists, and the need to perform multiple investigations to rule out conditions which can mimic ALS, lack of a diagnostic marker significantly contributes to diagnostic delay, which averages 1 year from symptom onset [1]. Given the rapidly progressing nature of ALS, this delay can have significant clinical and lifestyle impact on patients and limits recruitment of patients with early phase disease to clinical trials. With the potential for the approval of new therapies currently in different stages of clinical development over the coming years, there is a pressing need for a validated biomarker for the diagnosis of ALS.

While advances in genomic sequencing have provided new insights into the disease [2], gene sequencing is primarily used to assess familial risk and define biological subtypes in the 10% or so of patients carrying mutations once the clinical diagnosis of ALS has been established, and therefore does not in itself provide a way of improving early diagnosis [3]. Another approach that has been used to aid in diagnosis of other

* Corresponding author.
E-mail address: alexandre.akoulitchev@oxfordbiodynamics.com (A. Akoulitchev).

https://doi.org/10.1016/j.ebiom.2018.06.015

Research in context

Evidence Before this Study

We searched primary research studies done in human ALS subjects in the last ten years and referenced in PubMed by use of the MeSH terms "(amyotrophic lateral sclerosis OR ALS) AND (biomarker OR marker) AND (diagnostic OR diagnosis) AND (blood OR PBMC OR plasma OR serum) AND (sensitivity OR specificity OR AUC)". There were no language restrictions. We identified 16 studies where diagnostic biomarkers for ALS were determined in a non-invasive, clinically accessible biological sample and statistical power was reported. In these studies, eight used plasma as a biomarker source, five used serum and three studies used PBMCs or whole blood. The biomarkers ranged from mRNA, proteins/peptides, metabolites, metals, or combinations of several molecular modalities combined into a multi-marker panel. Neurofilament light (NfL) was the most extensively studied, and the sensitivity and specificity of the biomarkers in making a diagnosis of ALS ranged between 90 and 93% and 58–91%, respectively. Two studies showed no significant diagnostic power with the biomarkers under investigation.

Added Value of this Study

The current diagnosis of ALS remains mainly based on clinical parameters. However, the development of molecular tests can be used to exclude other diseases and help to confirm the diagnosis. Currently, there is a shortage of these molecular tests available to physicians. We were able to develop a highly discriminatory chromosome conformation signature that could accurately identify patients with ALS in an independent patient cohort. The test can be performed within a day on standard laboratory equipment, uses a readily accessible biofluid (blood) and requires and requires a minimal amount of volume.

Implications of all the Available Evidence

Our findings indicate that a simple and rapid blood-based test can distinguish patients with ALS from healthy controls with a high degree of sensitivity and can serve as a complementary tool in helping aid in disease diagnosis. These preliminary findings provide an initial proof of concept that the approach of looking at changes in genomic architecture provide a reliable readout of physiological changes associated with neurological disease. Additional studies that independently validate the biomarker panel identified here and assess the ability of the panel to discriminate ALS from other motor neuron diseases are required before application in pre-clinical and clinical settings.

neurological disorders is the analysis of non-sequence based alterations in the genome (epigenetics) [4, 5]. This is particularly useful in understanding the pathogenesis of multifactorial neurodegenerative diseases like ALS, where epigenetics can expose an integrated view of cellular function and dysfunction via regulation of gene expression [6].

The exploration of patient-derived samples is an obvious choice in attempting to discover new tools for diagnosing ALS, as biofluid collection is increasingly being done in clinical settings to serve as a data source for potential biomarkers. In light of this, the Northeast ALS Consortium (NEALS) Biofluid Repository was established to provide researches and industry partners with biologic samples collected from the patients using standard operating procedures (SOPs) and linked to clinical information for use in research studies [7]. In this pilot study, samples from the NEALS Biofluid Repository were analyzed using *EpiSwitch*, a high-resolution technology to identify structural-functional epigenetic changes in genomic architecture associated with pathological phenotypes developed by Oxford BioDynamics [8–13]. As multiple genomic regions contribute to phenotypic differences through changes in genomic architecture, this approach allows for the development of a chromosomal conformation signature (CCS) of alterations in genomic architecture between two states (disease vs. non-diseased, pre-treatment vs. post-treatment).

With the aim of identifying novel approaches to the diagnosis of ALS, this study was undertaken to discover and validate a CCS applicable to the diagnosis of ALS. After defining and refining a biomarker panel, we applied the signature to an independent sample cohort for validation. Last, the biological relevance in ALS of the top performing markers was assessed.

2. Methods

High-throughput screening of blood samples and a multi-step selection process was used to define a panel of epigenetic changes that could distinguish ALS patients from healthy patients.

2.1. Sample Collection

All samples banked and collected were done under IRB approved protocols (Oxford University samples: NRES Committee South West - Cornwall & Plymouth, reference 15/SW/0224). For the initial biomarker screening and development, the NEALS Biofluid Repository provided 50 ALS (Table 1) and 5 healthy control whole blood samples (Table 2). Oxford BioDynamics sample collection provided a further 37 controls (Table 2). In the validation stages of the project, Oxford University provided an independent sample cohort of eight ALS and eight spousal healthy control samples (Supplementary Table S1). Clinical characteristics for ALS patients were similar between the Discovery and Validation cohorts (Table 3). Whole blood samples were collected by peripheral venipucture using a 22-gauge large bore needle. Blood was collected directly into EDTA filled BD Vacutainer™ The tubes were immediately mixed by inversion and placed into a -80° C freezer. Samples were transported on dry ice and the frozen condition inspected on delivery.

2.2. Application of EpiSwitch and the Stepwise Biomarker Discovery Process

EpiSwitch is a high throughput technology platform that pairs high resolution chromosome conformational capture results with regression analysis and machine learning to develop disease classifications [8]. Screening and selection of statistically significant differences in conditional and stable profiles of genome architecture associated with samples from patients suffering from a disease, in comparison to healthy control samples, serves as a way to select epigenetic biomarkers that can diagnose and stratify pathological conditions [8–13]. In this study, *EpiSwitch* was used on blood samples in a three-step process to identify, evaluate, and validate statistically-significant differences in chromosomal conformations between ALS patients and healthy controls (Fig. 1).

An initial customized CGH Agilent microarray (8x60k) was designed to test technical and biological repeats for 13,880 potential chromosome conformations across 308 genetic loci. With the focus on the development of a non-invasive blood based diagnostic test, we first concentrated our attention on potential chromosome conformations in genomic loci specific to ALS's immuno-footprint. A literature search was conducted to identify loci that would be used on the microarray. In an earlier study, we compared and reported unique and common aspects of the ALS immuno-footprint to other Autoimmune Conditions

Table 1
NEALS Biofluid Repository samples used in this study.

Study	Sample ID	Basic Annotation	Sample Type	Gender	Ethnic Category	Race	Age at Diagnosis	Disease Duration (Month from Symptom Onset to Sample Collection)	ALSFRS Total Score	ALS Type
Skin biopsy	701001	ALS	Whole blood	Male	Non-Hispanic or Latino	White	67	34.20	38	Sporadic
	701002	ALS	Whole blood	Female	Non-Hispanic or Latino	White	42	22.51	24	Sporadic
	701024	ALS	Whole blood	Male	Non-Hispanic or Latino	White	67	15.9	42	Sporadic
	701026	ALS	Whole blood	Male	Non-Hispanic or Latino	White	35	31.11	41	Sporadic
	701028	ALS	Whole blood	Male	Non-Hispanic or Latino	Black	48	14.06	43	Sporadic
	701032	ALS	Whole blood	Female	Non-Hispanic or Latino	White	57	9.66	40	Familial
	701035	ALS	Whole blood	Male	Non-Hispanic or Latino	White	63	39.26	29	Sporadic
	701037	ALS	Whole Blood	Female	Non-Hispanic or Latino	White	49	15.28	40	Sporadic
	701040	ALS	Whole blood	Female	Non-Hispanic or Latino	White	39	19.52	43	Sporadic
	701043	ALS	Whole blood	Male	Non-Hispanic or Latino	White	50	7.92	29	Sporadic
	701054	ALS	Whole blood	Male	Non-Hispanic or Latino	White	44	16.99	39	Sporadic
	701060	ALS	Whole blood	Male	Non-Hispanic or Latino	White	46	3.02	42	Sporadic
	701080	ALS	Whole blood	Female	Non-Hispanic or Latino	White	66	12.65	36	Sporadic
	701021	ALS	Whole blood	Female	Non-Hispanic or Latino	White	64	13.96	17	Sporadic
ALS Sample repository	701001	ALS	Whole blood	Female	Non-Hispanic or Latino	White	57	13.57	N/A	Sporadic
	701026	ALS	Whole blood	Female	Non-Hispanic or Latino	White	47	0	N/A	Sporadic
	701027	ALS	Whole blood	Female	Non-Hispanic or Latino	White	55	0.4	N/A	Familial
	701038	ALS	Whole blood	Female	Non-Hispanic or Latino	White	73	0.92	N/A	Sporadic
	701042	ALS	Whole blood	Male	Non-Hispanic or Latino	White	56	8.76	N/A	Sporadic
	701043	ALS	Whole blood	Female	Non-Hispanic or Latino	White	59	10.61	N/A	Sporadic
	701044	ALS	Whole blood	Male	Non-Hispanic or Latino	White	58	1.5*	N/A	Sporadic
	701045	ALS	Whole blood	Male	Non-Hispanic or Latino	White	47	5.9	N/A	Sporadic
	701048	ALS	Whole blood	Female	Non-Hispanic or Latino	White	62	14	N/A	Sporadic
	701049	ALS	Whole blood	Female	Non-Hispanic or Latino	White	47	11	N/A	Sporadic
	701051	ALS	Whole Blood	Male	Non-Hispanic or Latino	White	65	26.23	N/A	Sporadic
	701052	ALS	Whole blood	Male	Non-Hispanic or Latino	White	46	63.26	N/A	Sporadic
	701055	ALS	Whole blood	Female	Non-Hispanic or Latino	White	55	2.1	N/A	Sporadic
	701056	ALS	Whole blood	Male	Non-Hispanic or Latino	White	53	0.43*	N/A	Sporadic
	701064	ALS	Whole blood	Female	Non-Hispanic or Latino	White	67	0.74*	N/A	Sporadic
	701066	ALS	Whole blood	Male	Non-Hispanic or Latino	White	41	9	N/A	Sporadic
	701069	ALS	Whole blood	Male	Non-Hispanic or Latino	White	51	0.48	N/A	Familial
	701082	ALS	Whole blood	Male	Non-Hispanic or Latino	White	52	11.36*	N/A	Sporadic
	701083	ALS	Whole blood	Male	Hispanic, Latino	White	55	50.26*	N/A	Sporadic
	701084	ALS	Whole blood	Male	Non-Hispanic or Latino	White	51	1.17	N/A	Sporadic
	701085	ALS	Whole blood	Male	Non-Hispanic or Latino	White	47	38.67*	N/A	Familial
	701101	ALS	Whole blood	Male	Non-Hispanic or Latino	Black	43	43.73*	N/A	Sporadic
	701107	ALS	Whole	Female	Non-Hispanic or	Unknown/Not	65	2.83	N/A	Familial

(continued on next page)

Table 1 (*continued*)

Study	Sample ID	Basic Annotation	Sample Type	Gender	Ethnic Category	Race	Age at Diagnosis	Disease Duration (Month from Symptom Onset to Sample Collection)	ALSFRS Total Score	ALS Type
			blood		Latino	reported				
	701108	ALS	Whole blood	Male	Non-Hispanic or Latino	White	70	0	N/A	Familiar
	701116	ALS	Whole blood	Male	Unknown/Not reported	Unknown/Not reported	68	3.89*	N/A	Sporadic
	701122	ALS	Whole blood	Male	Non-Hispanic or Latino	White	58	0.45	N/A	Sporadic
	701132	ALS	Whole blood	Female	Non-Hispanic or Latino	White	61	2.86*	N/A	Sporadic
	701136	ALS	Whole blood	Male	Non-Hispanic or Latino	White	53	18.86	N/A	Sporadic
	701139	ALS	Whole blood	Female	Non-Hispanic or Latino	White	47	7.03	N/A	Familial
	701142	ALS	Whole blood	Male	Unknown/Not reported	Unknown/Not reported	31	0	N/A	Sporadic
	701148	ALS	Whole blood	Male	Non-Hispanic or Latino	White	44	3.26	N/A	Sporadic
	701154	ALS	Whole blood	Male	Non-Hispanic or Latino	White	N/A	N/A	N/A	Disease Control
	701158	ALS	Whole blood	Male	Non-Hispanic or Latino	White	52	29.48	N/A	Sporadic
	701161	ALS	Whole blood	Male	Non-Hispanic or Latino	White	55	8.5	N/A	Sporadic
	701163	ALS	Whole blood	Male	Non-Hispanic or Latino	White	46	4.54*	N/A	Sporadic
	701185	ALS	Whole blood	Male	Non-Hispanic or Latino	White	43	108–120*	N/A	Sporadic
	701151	Healthy control	Whole blood	Female	Non-Hispanic or Latino	White	N/A	N/A	N/A	Healthy control
	701143	Healthy control	Whole blood	Male	Non-Hispanic or Latino	White	N/A	N/A	N/A	Healthy control
	701174	Healthy control	Whole blood	Female	Non-Hispanic or Latino	White	N/A	N/A	N/A	Healthy control
	701172	Healthy control	Whole blood	Male	Non-Hispanic or Latino	White	N/A	N/A	N/A	Healthy control
	701141	Healthy control	Whole blood	Female	Non-Hispanic or Latino	Asian	N/A	N/A	N/A	Healthy control

such as Systemic Lupus Erythematosus (SLE), Ulcerative Colitis (UC), Rheumatoid Arthritis (RA), Multiple Sclerosis (MS) and Relapse-Remitting MS (MSRR) [14]. The genetic loci selected for the array were genes primarily involved in immunodeficiency, adaptive and innate immune systems, and cytokine signaling (Table 4).

A comparative microarray analysis was conducted using samples from individual ALS patients from the NEALS Biofluid Repository and pooled healthy control samples. Array readouts were analyzed with linear regression modeling to select the 153 chromosomal interactions with the ability to best discriminate ALS from controls (Table 5).

For the second step, the evaluation stage, the 153 biomarkers selected from the array analysis were translated into *EpiSwitch*™ PCR based-detection probes and used in multiple rounds of biomarker evaluation on an increasing number of patient samples. PCR primers were selected according to their ability to distinguish between ALS and healthy controls. Exact Fisher's *P*-value, GLMNET (alpha 0.5, penalized score) and standard logistic modeling scores including Coef, SE, Wald S and P-value were used to select the top eight biomarkers (Table 6). This selected chromosomal-conformation signature-biomarker set was then tested on a known ($n = 74$) and a blinded cohort ($n = 16$). Principal component analysis was also used to determine abundance levels and to identify potential outliers (Fig. 2). With *EpiSwitch*, initial screens identify significant markers using a small subset of patient samples, while the larger sample cohort sizes in later screens provide the statistical power to allow for the results to more closely approximate real-world populations.

The sample cohort sizes in this study were progressively increased to enable selection of the optimal markers for discriminating ALS samples from healthy controls. Cohort sizes were statistically powered to a level of sensitivity and specificity needed for clinical application. More specifically, in the first screening series, six ALS and six healthy control samples were used. In the subsequent screening step, 24 ALS and 24 controls samples were used. For the final screening, a panel consisting of the eight top biomarkers (Table 6) was applied to a separate cohort of 74 samples from the NEALS Biofluid Repository and Oxford University. Statistical analysis was carried out on the final screen of the binary data results. (See Results, (Table 7)).

To further validate the ALS CCS, the panel was tested on a blinded, independent ($n = 16$) cohort of blood samples supplied by Oxford University. The results were analyzed using Bayesian Logistic modeling, *p*-value null hypothesis (Pr(>|z|) analysis, Fisher-Exact P test and Glmnet (Table 8).

Last, we explored the biological relevance of the biomarkers by using a second array with 171,408 potential chromosome conformations across 467 loci that were functionally related to ALS [15] (Table 9). The list of 150 top performing loci from this screen were uploaded to the Search Tool for the Retrieval of Interacting Genes/Proteins (STRING) database containing over 9 million known and predicted protein-protein interactions (https://string-db.org) to create a network of ALS regulation.

3. Results

3.1. Patient Clinical Characteristics

In order to develop, test and validate the CCS biomarker panel, we used blood samples from two main cohorts. The first cohort (Discovery)

Table 2
Healthy control blood samples provided by Oxford BioDynamics and the NEALS Consortium used in this study.

Sample type	Participant no	Date sample collected	Baseline diagnosis
Healthy control	10088	11/13/2013	NFG
	10917	9/20/2013	NFG
	14376	9/11/2013	NFG
	16345	12/2/2013	NFG
	16391	11/13/2013	NFG
	16771	11/18/2013	NFG
	17139	9/20/2013	NFG
	17152	12/6/2013	NFG
	17238	10/29/2013	NFG
	17265	10/24/2013	NFG
	17280	11/8/2013	NFG
	17328	11/15/2013	NFG
	17410	12/19/2013	NFG
	17411	1/17/2014	NFG
	17414	1/2/2014	NFG
	17415	1/10/2014	NFG
	17416	2/18/2014	NFG
	17417	2/4/2014	NFG
	17419	1/20/2014	NFG
	17422	1/6/2014	NFG
	17426	12/19/2013	NFG
	17427	1/15/2014	NFG
	17432	2/4/2014	NFG
	17433	1/10/2014	NFG
	17434	1/2/2014	NFG
	17445	1/2/2014	NFG
	17446	1/10/2014	NFG
	17447	1/10/2014	NFG
	17448	1/17/2014	NFG
	17449	1/27/2014	NFG
	17451	1/29/2014	NFG
	17452	2/4/2014	NFG
	17454	1/16/2014	NFG
	17456	1/21/2014	NFG
	17457	1/31/2014	NFG
	17459	2/10/2014	NFG
	17467	2/10/2014	NFG
	17480	2/11/2014	NFG
	17495	2/17/2014	NFG
	17508	2/19/2014	NFG
	17669	2/24/2014	NFG
	701141	12/5/2014	NEALS respository control
	701143	12/5/2014	NEALS respository control
	701151	12/5/2014	NEALS respository control
	701172	12/5/2014	NEALS respository control
	701174	12/5/2014	NEALS respository control

Abbreviations. NFG: Normal Fasting Glucose.

consisted of 50 ALS samples and 42 healthy controls provided by NEALS and Oxford BioDynamics. The second cohort (Validation) consisted of 16 samples (8 ALS and 8 healthy familial controls) provided by the University of Oxford. For the ALS patients, samples in both cohorts were sex matched (approximately 2/3 male and 1/3 female), with the majority of cases being sporadic ALS (84% in the Discovery Cohort and 75% in the Validation cohort) (Table 3). Average ALSFRS-R scores (35.9 in Discovery and 36.4 in Validation), average age at diagnosis (53.4 years in Discovery and 54.9 years in Validation) and disease duration (53.4 in Discovery and 54.9 in Validation) were similar in both cohorts (Table 3). Although ethnicity and race were not available for the Validation cohort, the vast majority of patients in the Discovery (90%) were non-Hispanic or Latino Whites.

Table 3
ALS clinical characteristics of the Discovery and Validation cohorts.

	Discovery cohort (*N* = 50)	Validation cohort (*N* = 8)
Gender		
Male (N, (%))	32 (64)	5 (63)
Female (N, (%))	18 (36)	3 (37)
Ethnicity		
Non-Hispanic or Latino	47	N/A
Hispanic, Latino	1	N/A
Unknown/not reported	2	N/A
Race		
White (N, (%))	45 (90)	N/A
Black (N, (%))	2 (4)	N/A
Unknown/not reported (N, (%))	3 (6)	N/A
ALS type		
Sporadic (N, (%))	42 (84)	6 (75)
Familial (N, (%))	8 (16)	2 (25)
Age at diagnosis (Average, (SD))	53.4 (9.7)	54.9 (11.9)
Disease duration (Average, (SD))	15.6 (20.4)	11.0 (7.9)
ALSFRS-R (Average, (SD))	35.9 (8.1)*	36.4 (7.7)

N/A = Not Available.
* ALSFRS-R scores were available for 14 of the 50 patients in the Discovery cohort.

3.2. Identity of the Markers in the Signature

The *EpiSwitch* three-step biomarker selection process yielded a distinct chromosome conformational disease classification signature for ALS comprised of chromosomal interactions in eight genomic loci. The loci contained in the signature are CD36, TAB2, GLYCAM1, GRB2, FYN, PTPRC, DNM3 and IKBKB (Table 6). The final ALS CCS was derived from high-throughput analysis using the *EpiSwitch* discovery platform initially identifying 153 potential biomarker interactions. Statistical analysis results from the binary data analysis are shown in Table 5.

3.3. Sensitivity and Specificity Analysis

The discriminating power of the ALS CCS are shown in Tables 6 and 7. Sensitivity and specificity for ALS detection in the 74 unblinded-tissue samples using the ALS CCS was 83·33% (CI 51·59 to 97·91%) and 76·92 (46·19 to 94·96%), respectively. In an independent, blinded cohort, sensitivity of the ALS CCS reached 87·50% (CI 47·35 to 99·68%) and specificity was 75·0% (34·91 to 96·81%).

3.4. Biological Relevance in ALS

When we mapped the markers in the ALS CCS to the Metacore™ signaling pathway database, the TLR2 and 4 signaling pathways showed significant enrichment with three genomic loci (CD36, TAB2 and IKBKB) mapping to this signaling cascade (Fig. 3). To acquire additional insights into how the loci identified in this study contribute to the pathophysiology of ALS, we expanded our analysis to include an array-based comparison of ALS patients versus healthy controls using a set of loci that have been previously associated with ALS as an initial screen. Based on comparison of 16 ALS patients and 16 controls, 150 statistically disseminating markers were identified (Table 9). Genetic loci enriched with significant epigenetic deregulation were used to build a protein regulatory network using the STRING database (Fig. 4). When analyzing the resulting network (Additional Files 1 and 2), key hubs included proteins with known links to the pathophysiology of ALS including SOD1, TARDBP (TDP-43), NEFH, and UBQLN2 [16–18] (Fig. 4). In addition to the well-studied loci with known links to ALS, the network analysis confirmed the involvement of emerging and lesser-studied genomic loci in

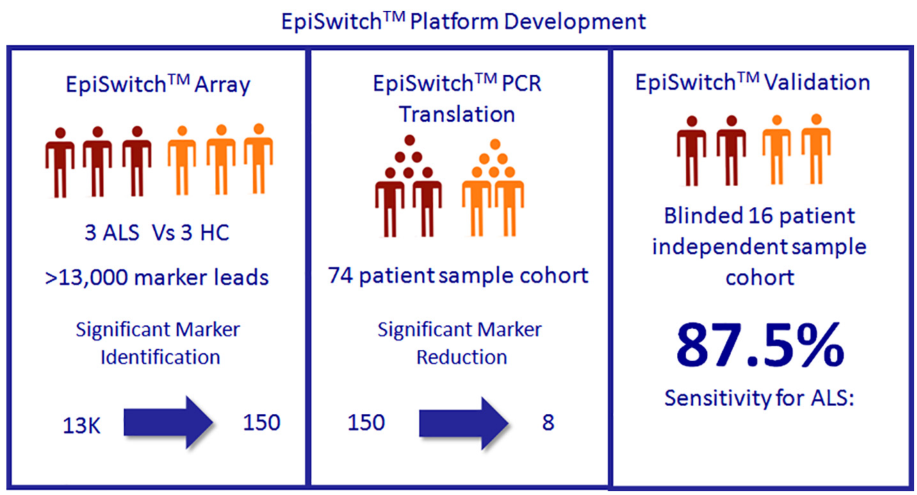

Fig. 1. Three-step biomarker discovery workflow. Starting with an initial pool of over 13,000 markers, a series of statistical comparisons between ALS and healthy controls samples refined the final ALS chromosome conformation signature panel into a set of 8 markers that could diagnose ALS patients in a blinded, independent cohort with 87.5% sensitivity.

the development of ALS including KIFAP3 which has been recently identified as a potential risk locus for ALS and GRIP1 which was shown to be altered in ALS2 deficient spinal motor neurons leading to neuronal degeneration [19–21]. This indicates that consistent epigenetic deregulation is observed in key genetic loci in the largely sporadic ALS patient population used in this study.

4. Discussion

For the majority of patients with ALS, the etiology of the disorder is unknown. Mutations in a number of genes such as: *C9orf72*, Cu, Zn superoxide dismutase 1 (SOD1) and TAR-DNA binding protein (TDP-43), found in familial ALS occur in only about 10% of the patient population [22–25]. Other studies suggest common pathogenic mechanisms for both the non-genetic and the genetic forms of ALS, as well as, similar clinical courses and dysfunctional features [2, 25]. A hexanucleotide expansion in the *C9orf72* gene is the most common genetic mutation [26, 27]. The discovery of the repeat expansion of the C9orf72 hexanucleotide provides bridge between familial ALS and sporadic ALS [27–29]. The mutation is detectable in about 40% of familial ALS patients and 8–10% of sporadic ALS. The rapidly progressive nature of ALS means any improvement in diagnosis would be of great value to patients, their families and the professionals who treat them.

Epigenetics is the conduit for interactions between the environment and the genome. Epigenetic regulation of the genome can be used to explain complex diseases especially in the absence of any genetic mutations or patterns to explain pathology [14]. The foundation for diagnostic biomarker discovery using epigenetic frameworks rests with the detection and validation of conditional chromosome conformational changes at genetic loci of interest. Discovery is feasible and possible because chromosomal conformation comprises the smallest unit of regulated genome-linked to phenotype and asserts a high-level of regulation [14]. The binary quality (either the change is there or not), high biochemical stability and other characteristics of conditional chromosomal conformations make these genomic interactions highly advantageous as a source for potential diagnostic biomarkers [14].

OBD's platform technology and methodology, *EpiSwitch*, employs chromosome conformation capture and algorithmic analysis to detect and define a panel of epigenetic differences capable of discerning between diseased tissue samples and healthy controls. In this study, we identified, defined and evaluated chromosome conformations as biologically-distinguishing markers that comprise the first example of a non-invasive blood-based epigenetic signature for ALS. The study also provides the first indication that chromosomal conformational biomarker discovery may also provide a way to explore pathogenic pathways and mechanisms. The top performing *EpiSwitch* chromosome conformation biomarker maps to CD36, which encodes a fatty acid transport protein and has been shown to be linked to mitochondrial function. CD36 is also involved in the Toll Like Receptor (TLR) 2 and TLR4 signaling pathways. These toll-like receptors are activated in microglia in response to damage-associated molecular patterns. Interestingly, microglia have been shown to have a protective effect in early stage motor neuron degeneration [30]. Four biomarkers (i.e., Fyn, GRB2, IKBKB and CD45) appear in the pathways that map to the Major Histocompatibility Complex (MHC). Fyn plays a key role in initiating myelination by myelin-forming glial cells [31]. Three biomarker proteins (CD36, TAB2, IKBKB) are involved in pathways associated with the innate immune system. The IKK kinase complex is found in the regulation of gene expression in response to neurotransmission [32]. The location of these biomarkers in key pathways regulating the immune response point to the involvement of neuroinflammatory mechanisms in the pathogenesis of the disease [33].

The findings reported here add an additional clinical tool to aid in ALS diagnosis and further increase understanding of the disease Support for those concepts can be found in the panel of biomarkers discovered during this investigation. The gene loci related to the biomarkers in the ALS CCS, and their protein products, feature in cellular pathways linked to the phenotypic manifestations of ALS including: fatty acid transport, mitochondrial dysfunction, and alterations in both immune function and glial activation. Future studies using this approach and assessing blood samples collected longitudinally can also be applied as a new approach to monitor disease progression. In fact, recent studies indicate that the prediction of progression in ALS is possible using a set of patient clinical data (e.g. ALSFRS-R, ALSFRS slope, Trunk sub-score, time since diagnosis, systolic blood pressure, predicted survival) [34, 35]. Although the clinical annotations available for many of the samples used in this study were limited, future analysis of samples from longitudinal studies using EpiSwitch in combination with clinical metadata analysis and predictive algorithms are warranted.

Additionally, the CCS identified during this investigation aligns with more recent evidence that points to the concept of non-cell-autonomous disease pathogenesis and the contribution of microglia in ALS [36]. A number of investigations have indicated that the cells lose their surveillance and neuro-protective capacity by switching from an activated neuroprotective to a neurodegenerative phenotype as the disease progresses. Under normal conditions microglia activation results in upregulation of MHC class 2 proteins involved in presentation of antigens to T lymphocytes. Microglia also express a diverse set of pattern recognition receptors, including TLRs, for sensing pathogen-associated

Table 4
List of immune-related genomic loci tested in the initial ALS array.

Gene name	Array probe count	Gene name	Array probe count	Gene name	Array probe count
VCAM1	10	IGHV3-23	13	CD40	7
RAP1A	332	IGHV1-46	2	CXADR	8
NRAS	12	TRAV19	5	IFNAR2	24
CD160	24	TRAC	12	IFNAR1	4
FCGR1A	23	ADCY4	10	IFNGR2	90
RFX5	24	LGALS3	7	DONSON	5
THEM4	88	RASGRP1	9	ICOSLG	12
IL6R	138	B2M	30	ICOSLG;AIRE	3
FCER1A	2	CIITA	4	ITGB2	14
FCER1G	24	PRKCB	415	VPREB1	1
FCGR2A	19	PDPK1	51	IGLV7-43	8
FCGR3A;FCGR2A	4	IL21R	56	IGLC3;IGLC7;IGLC2;IGLC1;IGLC6	2
FCGR3A	42	CD19	10	BCR	100
FCGR2B;FCGR3A	125	LAT	22	IGLL1	10
CD247	254	ITGAL	23	SEC14L3	12
SELL	52	ITGAM	54	CSF2RB	15
DNM3	1121	ADCY9	132	IL2RB	4
PTPRC	154	CDH1	154	MKL1	183
CHI3L1	38	PLCG2	221	TNFRSF13C	4
C4BPB	9	GINS2	27	IRAK2	38
C4BPB;C4BPA	10	TNFRSF13B	7	CBLB	51
C4BPA	35	CPD	61	CD96	159
CD55	33	AP2B1	44	CD200	26
CR2	15	ERBB2	6	CD200R1	9
CR1;CR2	6	PLD2	10	CD80	21
CR1	205	C1QBP	36	CD86	11
CD46	11	MRC2	51	ADCY5	153
CD34	70	CD300LB	5	ITGB5	63
DDOST	11	CD300E	10	NCK1	95
TLR5	53	GRB2	270	TRPC1	21
LYPLA2	30	GUCY2D	13	PLD1	201
AKT3	437	SIGLEC15	2	AP2M1	13
CLIC4	479	MALT1	32	IL1RAP	29
IFI6	116	CD226	15	IL5RA	11
PTAFR	49	ICAM1	9	MYD88	8
ATPIF1;PTAFR	14	ICAM1;ICAM4	1	CCR2	2
ATPIF1	24	DNM2	235	DAPP1	26
LCK	158	PRKCSH	31	NFKB1	27
BCL10	18	ACP5	23	TLR2	5
PIK3CD	191	JAK3	21	CD38	24
CHUK	15	RFXANK	33	TLR10	2
NFKB2	5	HCST	3	TLR1;TLR10	3
PPAPDC1A	19	TYROBP;HCST	5	TLR1	4
FGFR2	95	TYROBP	12	TLR1;TLR6	3
MRC1	23	MATK	27	KLB	27
ITGB1	29	AKT2	34	PDGFRA	69
IL2RA	7	AKT2;PLD3	6	KIT	32
PRKCQ	164	PLD3	23	TICAM2	12
FAS	16	CD79A	6	CD14	55
BLNK	35	MADCAM1	3	PDGFRB	18
PIK3AP1	210	PVR	8	CD74	6
AP2A2	20	PVRL2	43	FGFR4	28
NCAM1	43	PTGIR	42	PRLR	41
AMICA1	16	AP2S1	10	IL7R	14
CD3E	13	AP2A1	22	GHR	114
CD3G	3	SIGLEC16	10	CCNO	7
CD3D	2	SIGLEC14	3	IL6ST	24
CD3G;CD3D	1	LILRB2	2	CD180	1
CXCR5	13	LILRB1	10	PIK3R1	14
CBL	41	LILRB4	13	ADCY2	364
CRTAM	11	KIR2DL4;KIR3DL1;KIR2DL3	13	FYN	332
TIRAP	2	KIR2DL4;KIR3DL1	11	IFNGR1	15
CD81	3	KIR3DL1	4	TAB2	150
IFITM1;IFITM2	4	KIR2DL1;KIR2DL4;KIR3DL1;KIR2DL3	5	ULBP1	14
IFITM3	6	KIR2DS4;KIR3DL1	1	ULBP3	34
CD59	7	KIR2DS4;KIR3DL1;KIR3DL2	2	CCR6	11
CD44	24	C3	28	MICB	28
ART1	1	VAV1;C3	3	CFB	2
RAG1;TRAF6	8	VAV1	49	C4A	3
RAG1	46	IL1R2	5	C4B	1
RAG2;RAG1	10	IL1R1	56	AGER	7
RAG2	8	IL1RN	9	TAP2;TAP1	3
SIGIRR	1	RAPGEF4	195	TAP1	4
HRAS	14	ITGA4	1	TREM2	5
MS4A2	12	ITGAV	1	TREM1	9

(continued on next page)

Table 4 (*continued*)

Gene name	Array probe count	Gene name	Array probe count	Gene name	Array probe count
SCYL1	9	CD28	2	NCR2	5
PANX1	29	ICOS	10	LY86	54
KLRD1	53	IRS1	6	MAP3K7	2
KLRK1	3	PDCD1	2	EPHB4	30
UNG	18	ADCY3	30	CLEC5A	7
P2RX7	53	RASGRP3	41	CARD11	50
ORAI1	22	SOS1	177	ADCY1	30
KRAS	5	ACTR2	46	EGFR	209
RAPGEF3	15	CD8A	9	LAT2	9
ADCY6	7	CD8A;CD8B	14	CD36	127
ITGB7	6	CD8B	22	ADCY8	121
GLYCAM1	6	IGKV1-5	10	PPAPDC1B	26
ERBB3	2	IGKV3-7	7	FGFR1	7
CD4	57	IGKV3-11	3	IKBKB	18
RAP1B	33	IGKV3-15	10	LYN	179
FRS2	63	IGKV3-20	3	PAG1	73
AICDA	3	IGKV2-30	8	TLR4	10
KLRG1	15	IGKV1D-16	8	ANGPTL2	4
IRS2	1	MAL	3	DNM1	11
ARHGEF7	94	ADAM17	17	SH3GL2	101
KL	23	ZAP70	10	CLTA	110
RFXAP	26	SIRPB1	4	CD274	1
DLEU2	20	GINS1	39	PDCD1LG2	1
AKT1	18	TRIB3	21	SYK	25
CD40LG	3	PLCG1	12	BTK	8
IL3RA;CSF2RA	3	ADA	9	CSF2RA	25
IL3RA	15	IKBKG	2	TAB3	35
IRAK1	5	SH3KBP1	291	**Total**	**13,880**

molecular patterns and endogenous ligands derived from cellular injury.

In addition to the eight loci that make up the CCS, expanded array analysis and overlay of a STRING protein network with genetic loci enriched in epigenetic deregulation shows evidence for strong biological concordance with genetic cases based on familial SOD1, TDP-43 and UBQLN2 (ALS subtype 15) genetic variants [37]. Epigenetic deregulation of SOD1, TDP-43, ERBB4 (ALS19), UBQLN2, INSR– all present themselves as significant events related to ALS etiology in sporadic cases investigated in this study. In addition to the STRING network identifying interconnected nodes with known link to disease, the analysis is also useful in the identification of novel disease mechanisms for target discovery. For example, the most interconnected node in the network was the alpha subunit of Protein Kinase C (PRKCA) (Fig. 4). While a role for Protein Kinase C has been known for decades in ALS ([38, 39]), our results implicate a supportive role for the glutamate metabotropic receptors GRM3 and GRM7 as potential intermediaries that can serve as novel disease targets [40].

Some of the caveats associated with our findings are the relatively modest sample size and the clinical homogeneity of the samples. According to a recently published global epidemiology analysis of published studies, ALS affects approximately 100,000 people worldwide [41]. In this study, we used 50 ALS patient samples and 42 healthy controls to develop the CCS and validated the signature on an additional 16 samples (8 ALS and 8 healthy controls), which represents a very small fraction of global cases. It is important to note however, that historical studies seeking to identify fluid-based biomarkers of ALS diagnosis have been developed on the analysis of between 28 and 103 ALS patients and between 12 and 43 healthy controls [42], sample numbers that are within the range of this study. Perhaps more importantly is the relative homogeneity of the samples in this study. The patients in the discovery cohort were overwhelmingly (>90%) Non-Hispanic or Latino Whites. While in the United States it has been recognized that there is a higher rate of ALS among Whites, a recent analysis of worldwide ALS incidence confirms the observation that the disease can affect people from a wide range of racial and ethnic backgrounds [43, 44]. Future studies looking at larger patient sets and the inclusion of a greater diversity of ethnic representation are warranted. Last, it is important to acknowledge that the benefits and limitations of using any surrogate non-invasive readout in a liquid biopsy, including this study, remain an important point of inquiry. Interestingly, recent studies have demonstrated that while distinct differences in gene expression profiles are observed in different tissue and cellular types; epigenetic differences, from DNA methylation to histone modifications to high order chromatin structures, certain markers could show local synchronization across cellular types. This includes macrophages and dendritic cells involved in immune surveillance which show concordant epigenetic signals between the primary site of pathology and in surrogate blood-based readouts [8, 45]. The current understanding of this phenomenon involves the exosome-mediated resetting of selective targeted cellular populations, described as a horizontal transfer [46, 47]. This is particularly relevant to exosome-based transfer of non-coding RNA, such as miRNA, long implicated in epigenetic resetting of secondary cellular targets in peripheral blood and distant tissues and directly associated with resetting of specific chromosome conformations in individual cells. Further epigenetic-based biomarker studies and extended validation on independent cohorts will help to better understand the features of these observed systemic epigenetic sub-signatures.

Finally, we believe that epigenetic insights may help to provide biomarkers directly related to ALS. EMG and conductivity tests have increased the sensitivity of ALS diagnosis by providing the first biological information to inform ALS diagnosis. The sensitivity of our assay using patient samples approaches the sensitivity results reported using Awaji Criteria and those reported for CSF neurofilaments, another biomarker in development for diagnosing ALS [48, 49]. Ultimately, complex and heterogeneous diseases like ALS will require an integrative multi-omics approach to better characterize disease onset and progression and the results presented here offer an additional molecular approach to understand disease pathology.

One of the major challenges in the current clinical practice of diagnosing ALS is the time is takes to make a definitive diagnosis. Under the current “rule-out” paradigm, it can take months to confirm a diagnosis of ALS. In addition, many of the current tools for aiding a diagnosis are expensive and can themselves take days to

Table 5
Top 153 markers produced from the second array.

Probe	GeneLocus	logFC	AveExpr	t	P·Value	adj.P·Val	B	FC	FC_1	Binary
ACOXL_2_110997162_111004405_111109898_111117325_RF	ACOXL	0.3298921	0.3298921	11.076483	1.09E-09	1.62E-07	12.487822	1.256919	1.2569193	1
ACOXL_2_110704616_110714102_110875631_110879536_RF	ACOXL	0.3570591	0.3570591	9.638804	1.03E-08	7.06E-07	10.263069	1.280812	1.2808123	1
ADAMTS20_12_43377477_43383257_43480754_43482402_FR	ADAMTS20	−0.246307	−0.246307	−9.267993	1.91E-08	1.10E-06	9.6485602	0.843052	−1.186167	−1
ADAMTS20_12_43377477_43383257_43588948_43590670_FR	ADAMTS20	−0.322419	−0.322419	−6.16799	6.55E-06	7.78E-05	3.7882954	0.799728	−1.250425	−1
ALDH1A2_15_58325151_58334051_58485549_58488054_FR	ALDH1A2	0.345862	0.345862	13.477242	4.03E-11	2.85E-08	15.710641	1.27091	1.2709101	1
ALDH1A2_15_58325151_58334051_58452555_58457099_FR	ALDH1A2	0.3633487	0.3633487	13.188649	5.84E-11	3.35E-08	15.352222	1.286408	1.2864084	1
ALDH1A2_15_58325151_58334051_58538695_58540885_FF	ALDH1A2	0.3398615	0.3398615	7.222828	7.78E-07	1.61E-05	5.9304456	1.265635	1.2656351	1
ANKRD29_18_23664553_23665914_23692491_23699757_RR	ANKRD29	0.2493527	0.2493527	8.6194055	5.83E-08	2.37E-06	8.5308864	1.188674	1.1886737	1
ATXN7L1_7_105654123_105657510_105741521_105750599_FR	ATXN7L1	0.18956	0.18956	6.5975399	2.70E-06	3.98E-05	4.678643	1.140416	1.1404158	1
BANK1_4_101510635_101519668_101619789_101624381_RF	BANK1	−0.390246	−0.390246	−10.63806	2.11E-09	2.34E-07	11.83492	0.763	−1.310616	−1
BANK1_4_101476784_101489895_101732279_101733831_FF	BANK1	0.3134993	0.3134993	10.813911	1.62E-09	2.03E-07	12.099391	1.242718	1.2427183	1
BTBD11_12_107272037_107279968_107305640_107312061_FF	BTBD11	0.3569279	0.3569279	13.088383	6.65E-11	3.57E-08	15.225963	1.280696	1.2806959	1
C2CD2_21_41868909_41872387_41979620_41986582_FR	C2CD2	0.3304577	0.3304577	9.7178208	9.05E-09	6.41E-07	10.391775	1.257412	1.2574123	1
C6orf132_6_42104999_42110975_42124471_42126639_RR	C6orf132	−0.151906	−0.151906	−10.15532	4.48E-09	3.96E-07	11.090489	0.900061	−1.111036	−1
C6orf58_6_127480771_127483471_127600017_127604343_FR	C6orf58	−0.206941	−0.206941	−7.65767	3.38E-07	8.58E-06	6.7690901	0.866372	−1.154238	−1
CAMK1D_10_12516951_12526338_12633776_12637357_FF	CAMK1D	−0.363678	−0.363678	−8.185719	1.27E-07	4.23E-06	7.7521485	0.777181	−1.286702	−1
CAPN9_1_230738572_230739927_230752057_230757333_RR	CAPN9	−0.224589	−0.224589	−8.238209	1.15E-07	3.91E-06	7.8477638	0.855839	−1.168444	−1
CCDC3_10_12924962_12934165_13046815_13049059_FF	CCDC3	0.2758308	0.2758308	9.9013068	6.72E-09	5.34E-07	10.687663	1.210691	1.2106911	1
CD1A_1_158226961_158229550_158243613_158252050_FR	CD1A	0.179006	0.179006	4.472859	0.000266	0.001399	0.0795021	1.132104	1.1321036	1
CDH12_5_21870983_21872848_21898498_21914941_RF	CDH12	0.3146402	0.3146402	9.742694	8.69E-09	6.31E-07	10.432129	1.243701	1.2437014	1
CDK14_7_90936378_90943000_91140859_91158297_FF	CDK14	0.3051704	0.3051704	5.623921	2.08E-05	0.000189	2.6276939	1.235565	1.2355646	1
CDK14_7_90855907_90868783_90891759_90898655_FF	CDK14	0.3654475	0.3654475	7.6163383	3.65E-07	9.09E-06	6.6905099	1.288281	1.2882812	1
CELSR1_22_46424151_46427901_46457142_46458718_FF	CELSR1	0.1775237	0.1775237	7.5038883	4.52E-07	1.07E-05	6.4755148	1.130941	1.130941	1
CHAMP1_13_114265206_114269925_114317775_114320752_RR	CHAMP1	−0.230721	−0.230721	−5.754561	1.57E-05	0.000152	2.9095095	0.852209	−1.173421	−1
CHSY3_5_129929941_129937973_130119673_130124677_RF	CHSY3	0.2485594	0.2485594	8.4314793	8.14E-08	3.02E-06	8.1965796	1.18802	1.1880203	1
CHSY3_5_130104704_130115924_130186143_130190278_RR	CHSY3	0.4537319	0.4537319	14.076616	1.91E-11	1.93E-08	16.432119	1.369578	1.3695785	1
CNTN4_3_2273300_2281776_2314685_2325027_FR	CNTN4	0.3355172	0.3355172	15.964666	2.12E-12	1.04E-08	18.519694	1.26183	1.2618297	1
CNTNAP2_7_146728706_146734820_146785878_146792823_RF	CNTNAP2	−0.440614	−0.440614	−7.429603	5.21E-07	1.18E-05	6.332521	0.736821	−1.357182	−1
CTNNA3_10_66299269_66302507_66496211_66513003_FF	CTNNA3	−0.436585	−0.436585	−14.22858	1.58E-11	1.70E-08	16.610284	0.738882	−1.353396	−1
CTNNA3_10_66496211_66513003_66783614_66787250_RR	CTNNA3	−0.309997	−0.309997	−8.536173	6.76E-08	2.64E-06	8.3834114	0.806643	−1.239705	−1
CTNNA3_10_66282876_66290806_66496211_66513003_RR	CTNNA3	−0.309827	−0.309827	−5.790351	1.45E-05	0.000143	2.986383	0.806739	−1.239559	−1
CTNND2_5_11851889_11854697_11917286_11928978_FR	CTNND2	0.2692826	0.2692826	13.156667	6.09E-11	3.43E-08	15.312047	1.205208	1.2052083	1
DAO_12_108832598_108835352_108845485_108846981_FF	DAO	0.2606268	0.2606268	7.576059	3.94E-07	9.68E-06	6.6137018	1.197999	1.197999	1
DBF4B_17_44683672_44686134_44709459_44712660_RR	DBF4B	−0.269502	−0.269502	−8.674587	5.29E-08	2.23E-06	8.6281464	0.829606	−1.205391	−1
DGKB_7_14197847_14209024_14254130_14267710_FR	DGKB	−0.43638	−0.43638	−9.791092	8.03E-09	5.98E-07	10.51043	0.738986	−1.353205	−1
DGKB_7_14197847_14209024_14322087_14328928_FF	DGKB	−0.306194	−0.306194	−7.866591	2.28E-07	6.51E-06	7.162654	0.808772	−1.236442	−1
DIO2_14_80195869_80197807_80255209_80263592_RR	DIO2	−0.25104	−0.25104	−8.332113	9.73E-08	3.40E-06	8.0178794	0.84029	−1.190065	−1
DIO2_14_80255209_80263592_80371554_80373780_RR	DIO2	−0.307653	−0.307653	−13.98334	2.14E-11	1.99E-08	16.321825	0.807955	−1.237693	−1
DPP10_2_115459376_115465174_115685306_115694818_FR	DPP10	−0.327317	−0.327317	−8.420239	8.31E-08	3.06E-06	8.1764331	0.797017	−1.254678	−1
DPP10_2_114901417_114910472_115087678_115094206_FF	DPP10	0.3377111	0.3377111	14.406874	1.28E-11	1.51E-08	16.816949	1.26375	1.26375	1
DSCR4_21_37943561_37949090_38013989_38021392_FF	DSCR4	−0.429276	−0.429276	−12.81368	9.54E-11	4.43E-08	14.875361	0.742634	−1.346558	−1
ERBB4_2_212097934_212104780_212317329_212325591_RF	ERBB4	−0.315689	−0.315689	−4.50592	0.000247	0.001323	0.1537846	0.803467	−1.244606	−1
ERC1_12_1043264_1050801_1096484_1101318_FR	ERC1	0.233095	0.233095	13.553981	3.66E-11	2.79E-08	15.804721	1.175354	1.1753537	1
FAM126A_7_22873341_22878517_22945935_22949410_RF	FAM126A	−0.177613	−0.177613	−4.427145	0.000295	0.001522	−0.023251	0.884165	−1.131011	−1
FARP1_13_98271575_98282700_98346930_98348486_FR	FARP1	0.2548222	0.2548222	14.739287	8.58E-12	1.48E-08	17.195539	1.193189	1.1931887	1
FBXO8_4_174254227_174258882_174284851_174288977_RR	FBXO8	−0.339902	−0.339902	−6.993433	1.22E-06	2.24E-05	5.4774396	0.790095	−1.265671	−1
FER1L6_8_123963222_123969450_124085753_124093275_FR	FER1L6	0.350543	0.350543	5.6694435	1.88E-05	0.000175	2.726108	1.27504	1.2750404	1
FHIT_3_61064178_61073078_61136784_61147623_RR	FHIT	0.3193953	0.3193953	4.8524668	0.000113	0.000713	0.9299331	1.247807	1.2478074	1
FRMD3_9_83388882_83396653_83414350_83418756_FR	FRMD3	−0.383857	−0.383857	−11.50548	5.83E-10	1.14E-07	13.106219	0.766386	−1.304826	−1
GALNTL6_4_172641518_172647332_172893415_172910203_RF	GALNTL6	−0.310946	−0.310946	−14.25721	1.53E-11	1.70E-08	16.643649	0.806113	−1.240521	−1
GFPT1_2_69307499_69311057_69383954_69393165_FR	GFPT1	−0.317965	−0.317965	−6.644846	2.45E-06	3.70E-05	4.7752111	0.802201	−1.246571	−1
GFRA1_10_116092148_116100672_116113263_116118675_FR	GFRA1	−0.319379	−0.319379	−7.079082	1.03E-06	1.99E-05	5.6474303	0.801415	−1.247793	−1
GLIS3_9_3998831_4010284_4144132_4146272_FF	GLIS3	−0.309431	−0.309431	−6.997876	1.21E-06	2.23E-05	5.4862817	0.80696	−1.239219	−1
GMDS_6_2030214_2038438_2217079_2225905_RF	GMDS	−0.412681	−0.412681	−9.027894	2.87E-08	1.47E-06	9.2412584	0.751226	−1.331157	−1

(continued on next page)

Table 5 (*continued*)

Probe	GeneLocus	logFC	AveExpr	t	P·Value	adj.P·Val	B	FC	FC_1	Binary
GPC6_13_93573654_93584189_93748106_93754722_RF	GPC6	0.316254	0.316254	11.287633	8.00E-10	1.32E-07	12.794673	1.245093	1.2450934	1
GRIK2_6_101912977_101914543_101980061_101996881_FF	GRIK2	−0.412403	−0.412403	−10.64034	2.11E-09	2.34E-07	11.838361	0.751371	−1.330901	−1
GRIP1_12_66761739_66764959_66791577_66801892_RR	GRIP1	−0.333991	−0.333991	−10.33187	3.39E-09	3.23E-07	11.365922	0.793339	−1.260496	−1
GRM3_7_86653882_86655924_86695387_86706974_RF	GRM3	−0.311021	−0.311021	−9.568226	1.16E-08	7.66E-07	10.147448	0.806071	−1.240585	−1
GRM7_3_6827121_6836161_7047731_7057814_RR	GRM7	−0.359722	−0.359722	−7.091136	1.01E-06	1.96E-05	5.6712713	0.779315	−1.283179	−1
HCFC2P1_13_108440737_108444674_108461634_108471282_RR	HCFC2P1	0.3137758	0.3137758	11.555559	5.42E-10	1.09E-07	13.177127	1.242957	1.2429565	1
HCFC2P1_13_108440737_108444674_108461634_108471282_FR	HCFC2P1	0.329425	0.329425	11.346554	7.34E-10	1.27E-07	12.879437	1.256513	1.2565125	1
HDAC4_2_239204078_239210374_239360246_239368872_FR	HDAC4	0.3383322	0.3383322	7.5918458	3.83E-07	9.44E-06	6.6438323	1.264294	1.2642941	1
HPGD_4_174493630_174502964_174542132_174543999_RF	HPGD	0.1857242	0.1857242	11.142003	9.91E-10	1.53E-07	12.583558	1.137388	1.1373878	1
HUS1_7_47823192_47830325_47842954_47848362_RF	HUS1	−0.174947	−0.174947	−4.911921	9.92E-05	0.000643	1.0624681	0.8858	−1.128923	−1
IL1A_2_112795355_112798834_112816387_112823836_RR	IL1A	−0.103722	−0.103722	−3.037051	0.006829	0.019309	−3.100991	0.930629	−1.074542	−1
IL1A_2_112765786_112772711_112810765_112813086_RR	IL1A	0.1305595	0.1305595	3.6789915	0.001613	0.006001	−1.701299	1.094718	1.0947181	1
INSR_19_7099584_7101451_7138185_7142897_RF	INSR	0.1639687	0.1639687	10.303077	3.55E-09	3.32E-07	11.321255	1.120365	1.1203649	1
IQGAP2_5_76698020_76702533_76717099_76725306_FF	IQGAP2	−0.310676	−0.310676	−10.6174	2.18E-09	2.39E-07	11.803605	0.806264	−1.240289	−1
IQGAP2_5_76475531_76481400_76717099_76725306_FR	IQGAP2	0.2854775	0.2854775	11.70784	4.36E-10	9.61E-08	13.391129	1.218814	1.2188136	1
KCNMA1_10_77411418_77416164_77530837_77543678_RF	KCNMA1	0.3281284	0.3281284	8.0962784	1.49E-07	4.77E-06	7.5883505	1.255384	1.2553837	1
KCNN2_5_114353357_114360896_114430044_114433040_RR	KCNN2	−0.232264	−0.232264	−7.774872	2.71E-07	7.34E-06	6.9906211	0.851298	−1.174677	−1
KCNS3_2_17835106_17846049_17968712_17974054_FR	KCNS3	−0.288729	−0.288729	−11.37806	7.01E-10	1.24E-07	12.924607	0.818623	−1.221564	−1
KIAA0513_16_85000072_85002703_85074194_85077477_RF	KIAA0513	0.2060683	0.2060683	5.4679401	2.91E-05	0.000245	2.2888169	1.15354	1.1535402	1
KIFAP3_1_169911687_169919606_169986992_169993331_FR	KIFAP3	0.2934999	0.2934999	11.698018	4.42E-10	9.62E-08	13.377399	1.22561	1.22561	1
LINGO2_9_28333777_28339631_28527863_28540481_FR	LINGO2	−0.374728	−0.374728	−9.390644	1.55E-08	9.38E-07	9.8537519	0.771251	−1.296595	−1
LINGO2_9_28314155_28333777_28522753_28525112_FR	LINGO2	−0.463013	−0.463013	−7.06033	1.07E-06	2.04E-05	5.6102993	0.72547	−1.378417	−1
LINGO2_9_28314155_28333777_28510932_28517950_FF	LINGO2	−0.352913	−0.352913	−2.842326	0.010477	0.027372	−3.509391	0.783001	−1.277137	−1
LYPD3_19_43451257_43453307_43494229_43495321_FR	LYPD3	−0.108357	−0.108357	−3.699682	0.001539	0.005775	−1.655267	0.927644	−1.078	−1
MACROD2_20_15750414_15763248_15953272_15965024_RF	MACROD2	−0.439686	−0.439686	−10.55166	2.41E-09	2.56E-07	11.703674	0.737295	−1.356309	−1
MAGI2_7_78371356_78378740_78502868_78511891_FR	MAGI2	−0.309137	−0.309137	−7.781863	2.67E-07	7.28E-06	7.003776	0.807124	−1.238966	−1
MAGI2_7_79009346_79018304_79275810_79284623_RF	MAGI2	0.349446	0.349446	10.577281	2.32E-09	2.48E-07	11.742684	1.274071	1.2740713	1
MDGA2_14_47087312_47092151_47301555_47314511_FR	MDGA2	−0.376564	−0.376564	−2.53523	0.020267	0.046875	−4.13055	0.77027	−1.298246	−1
MGLL_3_127731924_127736779_127863699_127870283_RF	MGLL	−0.174384	−0.174384	−4.247058	0.000443	0.002114	−0.428303	0.886146	−1.128482	−1
NAV2_11_19476194_19490077_19749138_19755031_FR	NAV2	0.3411694	0.3411694	9.3822413	1.57E-08	9.44E-07	9.839756	1.266783	1.266783	1
NCKAP5_2_133209962_133217496_133394726_133400754_FF	NCKAP5	−0.363475	−0.363475	−8.42102	8.30E-08	3.06E-06	8.1778322	0.77729	−1.286521	−1
NCKAP5_2_133084614_133091683_133242680_133249277_RR	NCKAP5	0.3800747	0.3800747	11.195242	9.16E-10	1.46E-07	12.661003	1.301409	1.3014092	1
NEFH_22_29442588_29445314_29482081_29484217_RR	NEFH	0.1558858	0.1558858	12.070176	2.62E-10	7.50E-08	13.89074	1.114105	1.1141054	1
NEFH_22_29467180_29469328_29482081_29484217_FR	NEFH	0.3600069	0.3600069	5.6898359	1.80E-05	0.000169	2.7701205	1.283432	1.283432	1
NEFH_22_29434926_29438399_29467180_29469328_RF	NEFH	0.3191557	0.3191557	5.4943817	2.75E-05	0.000235	2.3464398	1.2476	1.2476002	1
NEIL3_4_177308770_177311798_177363195_177365833_RR	NEIL3	−0.440388	−0.440388	−4.173407	0.000524	0.00242	−0.593968	0.736936	−1.356969	−1
NELL1_11_21419712_21428422_21531472_21542215_RR	NELL1	−0.312849	−0.312849	−9.035358	2.83E-08	1.46E-06	9.2540329	0.805051	−1.242158	−1
NFIA_1_60869920_60875614_60989414_60996659_RR	NFIA	0.3492172	0.3492172	14.019512	2.04E-11	1.98E-08	16.364679	1.273869	1.2738693	1
NFIA_1_61228266_61235258_61246134_61250763_RF	NFIA	0.3172619	0.3172619	12.061499	2.65E-10	7.53E-08	13.87893	1.245964	1.2459636	1
NHSL1_6_138480977_138485998_138514855_138523394_RF	NHSL1	0.2467506	0.2467506	7.5585632	4.08E-07	9.94E-06	6.5802688	1.186532	1.1865317	1
NOX4_11_89337353_89346448_89499668_89503122_RF	NOX4	−0.321336	−0.321336	−12.36707	1.74E-10	6.04E-08	14.290321	0.800328	−1.249487	−1
NXPH1_7_8466580_8469680_8501926_8510453_FR	NXPH1	−0.343359	−0.343359	−9.44196	1.42E-08	8.81E-07	9.9390318	0.788204	−1.268707	−1
OPCML_11_133291292_133302754_133378245_133382756_FR	OPCML	−0.380902	−0.380902	−12.74907	1.04E-10	4.70E-08	14.791885	0.767957	−1.302156	−1
OSBP2_22_30729329_30730970_30763180_30773593_RR	OSBP2	−0.432395	−0.432395	−14.48833	1.16E-11	1.51E-08	16.910523	0.741031	−1.349472	−1
OSBP2_22_30729329_30730970_30817623_30822792_RR	OSBP2	−0.366312	−0.366312	−11.45424	6.28E-10	1.19E-07	13.033392	0.775763	−1.289053	−1
PA2G4P4_3_156818917_156822698_156846218_156854773_RR	PA2G4P4	−0.174657	−0.174657	−5.663311	1.91E-05	0.000177	2.7128629	0.885978	−1.128696	−1
PACRG_6_163022776_163030350_163324239_163328316_RR	PACRG	−0.352275	−0.352275	−9.207722	2.11E-08	1.20E-06	9.547019	0.783348	−1.276572	−1
PARVB_22_43989557_43996453_44182513_44187012_FF	PARVB	−0.170178	−0.170178	−7.603815	3.74E-07	9.26E-06	6.6666544	0.888733	−1.125198	−1
PASD1_X_151600201_151608969_151676020_151678489_RF	PASD1	0.3220619	0.3220619	5.8035886	1.41E-05	0.00014	3.0147787	1.250116	1.2501159	1
PASD1_X_151608969_151613880_151648877_151652329_RR	PASD1	0.3167815	0.3167815	2.5872149	0.018153	0.042868	−4.027661	1.245549	1.2455488	1
PLCB1_20_8599928_8617739_8698163_8700449_FR	PLCB1	−0.364492	−0.364492	−11.16982	9.51E-10	1.49E-07	12.624056	0.776742	−1.287428	−1
PLCB1_20_8599928_8617739_8856413_8858679_FF	PLCB1	−0.316603	−0.316603	−8.251608	1.13E-07	3.85E-06	7.8721116	0.802958	−1.245395	−1
PLEKHM3_2_207850576_207856308_208003089_208006543_FF	PLEKHM3	−0.385734	−0.385734	−8.300103	1.03E-07	3.58E-06	7.9600253	0.76539	−1.306524	−1
PON2_7_95405100_95420940_95465337_95474032_FR	PON2	−0.178367	−0.178367	−5.268811	4.50E-05	0.000344	1.8526765	0.883703	−1.131602	−1
PPP2R5E_14_63423316_63431065_63511598_63515339_FF	PPP2R5E	0.3121838	0.3121838	7.9196338	2.07E-07	6.02E-06	7.2616101	1.241586	1.2415857	1
PRKCA_17_66441276_66447067_66475597_66481312_RF	PRKCA	0.2425179	0.2425179	7.4515733	5.00E-07	1.15E-05	6.3748921	1.183056	1.1830556	1
PTPRD_9_9798181_9808250_9882262_9891784_RR	PTPRD	−0.453093	−0.453093	−4.232884	0.000458	0.002168	−0.460189	0.730475	−1.368972	−1

PTPRD_9_9551379_9564487_9756141_9761726_RF	PTPRD	0.3282945	0.3282945	10.781263	1.70E-09	2.09E-07	12.050556	1.255528	1.2555283	1
RAP1GAP2_17_2837827_2840795_2974137_2976800_RF	RAP1GAP2	−0.145079	−0.145079	−4.529412	0.000234	0.001268	0.2065487	0.90433	−1.105791	−1
RERGL_12_18254365_18255916_18350532_18364514_RF	RERGL	0.5204704	0.5204704	17.245127	5.42E-13	8.31E-09	19.793409	1.434423	1.4344229	1
RNF6_13_26220822_26221931_26255215_26259295_RR	RNF6	0.3776285	0.3776285	8.7845474	4.37E-08	1.95E-06	8.8207418	1.299204	1.2992044	1
RNU6-1264P_17_6162286_6163870_6195952_6199184_FR	RNU6-1264P	−0.152642	−0.152642	−9.038985	2.81E-08	1.46E-06	9.2602376	0.899602	−1.111603	−1
RORA_15_60977475_60986445_61019417_61030714_RR	RORA	0.3713685	0.3713685	14.275336	1.50E-11	1.70E-08	16.664729	1.293579	1.2935793	1
RPL9P15_3_154664590_154668268_154687949_154695597_RF	RPL9P15	0.2007438	0.2007438	5.5395118	2.49E-05	0.000218	2.4446246	1.149291	1.1492908	1
SCNN1B_16_23299279_23301635_23325818_23330880_FF	SCNN1B	−0.143058	−0.143058	−6.057416	8.25E-06	9.28E-05	3.5552838	0.905598	−1.104243	−1
SETBP1_18_44770146_44772357_44885635_44895879_RF	SETBP1	0.355569	0.355569	11.916137	3.25E-10	8.20E-08	13.679971	1.27949	1.2794901	1
SETBP1_18_44885635_44895879_45067644_45082246_FR	SETBP1	0.3703696	0.3703696	11.300548	7.85E-10	1.31E-07	12.813285	1.292684	1.2926839	1
SLC9A8_20_49784052_49786161_49876581_49883310_RR	SLC9A8	0.1512545	0.1512545	7.2660355	7.15E-07	1.50E-05	6.0149546	1.110535	1.1105347	1
SOD1_21_31645974_31648479_31675373_31681286_RF	SOD1	−0.11317	−0.11317	−2.698249	0.014316	0.03529	−3.804687	0.924554	−1.081602	−1
SORCS2_4_7241158_7248673_7449931_7456800_FR	SORCS2	0.3595133	0.3595133	10.619505	2.18E-09	2.39E-07	11.806804	1.282993	1.282993	1
SPAG16_2_213413840_213427575_213513566_213522278_FF	SPAG16	−0.390916	−0.390916	−12.83763	9.25E-11	4.35E-08	14.906206	0.762645	−1.311225	−1
SPTLC3_20_13133531_13136394_13174631_13182869_FF	SPTLC3	0.2023548	0.2023548	12.546312	1.36E-10	5.33E-08	14.527397	1.150575	1.1505748	1
STX7_6_132435332_132445259_132542354_132547678_FR	STX7	0.3463849	0.3463849	12.466212	1.52E-10	5.81E-08	14.421833	1.271371	1.2713708	1
STX7_6_132435332_132445259_132511475_132513451_FR	STX7	0.3187939	0.3187939	10.825435	1.59E-09	2.01E-07	12.116602	1.247287	1.2472874	1
SYN3_22_32593146_32596862_32844795_32854272_RF	SYN3	0.3341746	0.3341746	17.115411	6.20E-13	8.31E-09	19.669129	1.260656	1.2606559	1
SYN3_22_32723620_32730327_32844795_32854272_RF	SYN3	0.3345379	0.3345379	11.01189	1.20E-09	1.70E-07	12.392979	1.260973	1.2609735	1
TANGO6_16_68932310_68938132_69047292_69051982_FF	TANGO6	0.1825419	0.1825419	6.0822581	7.83E-06	8.95E-05	3.6077649	1.134882	1.1348817	1
TANGO6_16_68852020_68856905_68932310_68938132_RF	TANGO6	0.3129309	0.3129309	9.4084105	1.51E-08	9.16E-07	9.8833156	1.242229	1.2422288	1
TARDBP_1_10989562_10991726_11014552_11017016_FF	TARDBP	−0.096493	−0.096493	−5.268967	4.50E-05	0.000344	1.8530201	0.935304	−1.069171	−1
THSD7A_7_11420798_11426394_11712489_11724603_RF	THSD7A	0.3135925	0.3135925	7.2665721	7.14E-07	1.50E-05	6.0160025	1.242799	1.2427986	1
TMTC1_12_29532107_29533497_29647358_29657646_RF	TMTC1	0.3355121	0.3355121	11.641723	4.79E-10	1.00E-07	13.298511	1.261825	1.2618252	1
TMTC1_12_29647358_29657646_29765279_29767497_FF	TMTC1	0.3639387	0.3639387	3.4118158	0.002954	0.009869	−2.291571	1.286935	1.2869345	1
TP63_3_189677768_189688253_189719534_189721726_FR	TP63	−0.179873	−0.179873	−6.360572	4.39E-06	5.73E-05	4.1904365	0.88278	−1.132784	−1
UBQLN2_X_56536168_56538402_56553450_56557221_FR	UBQLN2	0.2784451	0.2784451	3.1075781	0.00584	0.016979	−2.950784	1.212887	1.212887	1
UBQLN2_X_56536168_56538402_56570114_56575112_RR	UBQLN2	0.3839068	0.3839068	3.3139007	0.003682	0.011761	−2.505503	1.304871	1.3048707	1
UBQLN2_X_56536168_56538402_56570114_56575112_FF	UBQLN2	0.3937521	0.3937521	3.2929041	0.00386	0.012196	−2.551177	1.313806	1.3138058	1
UBQLN2_X_56536168_56538402_56570114_56575112_FR	UBQLN2	0.3538926	0.3538926	2.693743	0.014455	0.035577	−3.813818	1.278004	1.2780042	1
VSNL1_2_17493823_17506407_17651961_17655968_FR	VSNL1	0.3086278	0.3086278	8.9568305	3.24E-08	1.60E-06	9.1192635	1.238529	1.2385291	1
WBSCR17_7_71656523_71666682_71682593_71686909_FR	WBSCR17	0.2893541	0.2893541	8.541732	6.69E-08	2.63E-06	8.3932893	1.222093	1.222093	1
WWOX_16_78559412_78566930_78777764_78783921_FF	WWOX	−0.312268	−0.312268	−7.888672	2.19E-07	6.31E-06	7.203896	0.805375	−1.241658	−1
XRCC1_19_43573185_43575618_43595713_43600345_RF	XRCC1	−0.126515	−0.126515	−7.497073	4.58E-07	1.08E-05	6.4624281	0.916042	−1.091653	−1
XRCC1_19_43573185_43575618_43595713_43600345_FR	XRCC1	0.1880671	0.1880671	8.9348232	3.36E-08	1.63E-06	9.0813491	1.139236	1.1392364	1
ZBTB20_3_114403907_114406568_114458618_114478185_RR	ZBTB20	−0.370005	−0.370005	−11.36464	7.15E-10	1.25E-07	12.90538	0.77378	−1.292358	−1
ZFPM2_8_105632010_105638904_105814873_105824107_FR	ZFPM2	−0.425339	−0.425339	−10.49363	2.64E-09	2.70E-07	11.615048	0.744664	−1.342888	−1
ZFPM2_8_105525568_105531254_105736941_105746180_RR	ZFPM2	−0.360993	−0.360993	−3.724595	0.001455	0.005518	−1.599789	0.778628	−1.28431	−1
ZFPM2_8_105572686_105580151_105814873_105824107_FR	ZFPM2	−0.324519	−0.324519	−3.057007	0.006534	0.018627	−3.058604	0.798565	−1.252247	−1
ZNF804B_7_88937416_88946263_88973548_88984178_RR	ZNF804B	0.3913267	0.3913267	16.279963	1.50E-12	1.04E-08	18.843266	1.311599	1.311599	1
PDE4B_1_66194325_66201588_66342345_66350066_RF	PDE4B	−0.283024	−0.283024	−6.650398	2.43E-06	3.67E-05	4.7865237	0.821866	−1.216743	−1

Abbreviations. logFC: logarithm of the fold change; AveExpr: Average expression; adj.P·Val: Adjusted *p*-value; B: B-statistic (log-odds that that gene is differentially expressed); FC: Fold change; FC_1: Fold change centered around 1; Binary: Binary call for loop presence/absence.

Table 6
The genomic loci contained in the chromosome conformation signature (CCS) used to inform an ALS diagnosis.

Gene	Fisher's *P* value	Coefficient	SE
CD36	0.003	−1.7788	0.8
TAB2	0.098	−0.8568	0.94
GLYCAM1	0.213	−0.9582	0.94
GRB2	0.055	−0.811	0.91
FYN	0.276	−2.0869	0.93
PTPRC	0.027	−1.7059	1.42
DNM3	0.142	−2.0227	0.92
IKBKB	0.117	−1.395	1.32

Abbreviations. SE: Standard error.

Table 7
Sensitivity and specificity of the ALS chromosome conformation signature (CCS) when used to classify a set of clinical samples (n = 74) taken from two ALS clinical trials.

Statistic	Value	95% CI
Sensitivity	0.8333	51.59% to 97.91%
Specificity	0.7692	46.19% to 94.96%
Positive likelihood ratio	3.61	1.30 to 10.06
Negative likelihood ratio	0.22	0.06 to 0.79
Disease prevalence	48% (*)	27.80% to 68.69%
Positive predictive value	76.92% (*)	46.19% to 94.96%
Negative predictive value	83.33% (*)	51.59% to 97.91%

Abbreviations. 95% CI: 95% confidence interval.

Table 8
Results from classification of blinded Oxford University samples (N = 16).

Statistic	Value	95% CI
Sensitivity	0.875	47.35% to 99.68%
Specificity	0.75	34.91% to 96.81%
Positive likelihood ratio	3.5	1.02 to 11.96
Negative likelihood ratio	0.17	0.03 to 1.09
Disease prevalence	50% (*)	24.65% to 75.35%
Positive predictive value	77.78% (*)	39.99% to 97.19%
Negative predictive value	85.71% (*)	42.13% to 99.64%

Abbreviations. 95% CI: 95% confidence interval.

weeks to interpret. The ALS CCS described here is based on simple, inexpensive and well-accepted molecular biology techniques and technical readouts are available within 24 h, offering a substantial time and cost savings to physicians and payors. While the application of the ALS CCS in the clinical setting will require further investigation, the potential use of a chromosome conformation signature to diagnose ALS from a simple to collect, non-invasive biofluid and simple, rapidly available clinical readouts available to physicians and caregivers promise to help fill the gap in the current methods for diagnosing ALS.

Supplementary data to this article can be found online at https://doi.org/10.1016/j.ebiom.2018.06.015.

Acknowledgements

Oxford BioDynamics would like to thank Barbara Nasto for her assistance in the preparation of this manuscript, which was funded by Oxford BioDynamics.

Oxford BioDynamics holds ethical approval information for all patient samples. Oxford University holds written consents for individual patient samples. Consents for NEALS Biofluid Repository samples are held at NEALS Biofluid Repository.

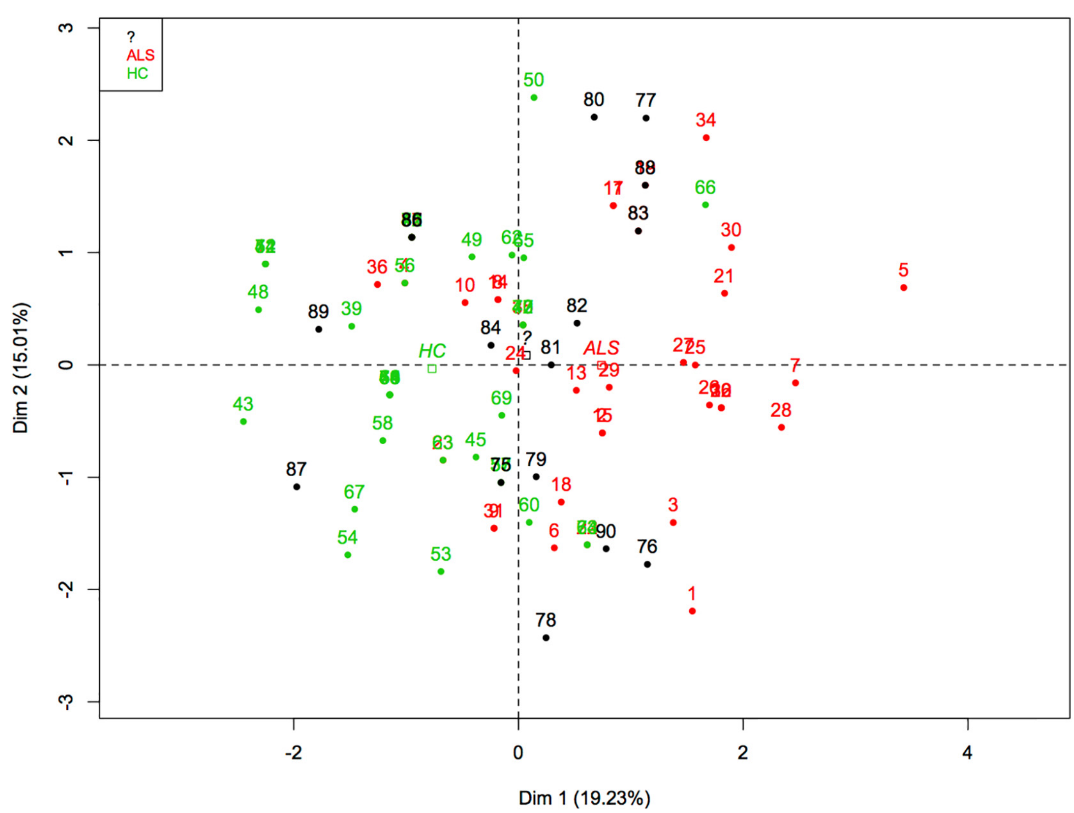

Fig. 2. Principal component analysis for the 8 markers applied to 74 known samples (ALS samples in red and healthy controls (HC) in green) and 16 unknown blinded samples (black). The blinded samples appear as a mixture of ALS and control samples.

Table 9
Loci that are functionally related to ALS used for the second array.

Gene name					
DPP6	AGBL1	DNAH2	KCNN3	RAMP3	ZMYND8
C9orf72	AGPAT5	DNAH9	KCNQ1	RAP1GAP2	ZNF407
ITPR2	AK8	DOCK8	KDM4B	RAPGEF4	ZNF423
UNC13A	AKAP6	DOCK9	KDR	RAPGEF5	ZNF485
MOB3B	AKAP7	DPF3	KIAA0040	RBFOX3	ZNF519
ALS2	AMD1	DPP10	KIAA0513	RDH14	ZNF710
CDH13	ANG	DSC3	KIAA1644	RERGL	ZNF804B
SOD1	ANKDD1A	DSCR4	KLHL29	RETSAT	
ALK	ANKRD29	DSTNP5	KLHL38	RGS17	
BARD1	ANKS1B	E2F7	KRT18P3	RNA5SP142	
BTBD11	ANO1	ELK3	KRT18P64	RNA5SP158	
FAM19A5	ANXA5	ELMSAN1	KSR2	RNF14	
GRIP1	AP2A2	ELP3	LAMA3	RNF17	
MACROD2	APBB2	EN1	LHFP	RNF6	
RBFOX1	APP	EPB41L3	LINGO2	RNGTT	
SHROOM3	ARHGEF3	ERG	LIPC	RNU6-1264P	
TARDBP	ARMS2	ERGIC1	LMO2	RNU6-242P	
AGAP1	ARNT2	ERMARD	LOX	RNU6ATAC32P	
AGBL4	ARSG	ESRRG	LRIG1	RORA	
ALDH1A2	ASIC2	EVC2	LRP1B	RPF2	
ATP2C2	ATP2A3	EXO1	LSAMP	RPL9P15	
ATXN2	ATXN1	EXOC2	LYPD3	RSPO4	
BANK1	ATXN7L1	EYA1	MAPK1	SAMD5	
BTBD16	AVEN	FAM126A	MAST4	SARM1	
CACNA2D3	B4GALT6	FAM13B	MDGA2	SCN8A	
CALN1	BCL6	FAM149A	MED13L	SCNN1B	
CDC42BPA	BEND7	FAM155A	MGLL	SETBP1	
CHSY3	BMPR2	FAM169B	MICAL3	SEZ6L	
CNTN6	BTLA	FAM189A1	MICB	SGMS1	
CNTNAP2	C15orf32	FAM194B	MKL2	SGSM1	
CSMD1	C2CD2	FBXO32	MKLN1	SHISA3	
DAB1	C4orf19	FER	MORN5	SIGLEC12	
DIO2	C6orf132	FER1L6	MTMR7	SIRPG	
DNM1L	C6orf58	FGF1	MTUS2	SLC24A2	
DOCK1	C7orf57	FGF12	MUC6	SLC35A3	
DSCAM	C8orf47	FGGY	MYH11	SLC35F3	
ERBB4	C9orf170	FHDC1	MYO10	SLC41A1	
ERC1	CABIN1	FHIT	MYO18B	SLC9A8	
FARP1	CADM2	FHOD3	MYO1D	SLIT3	
FBXO8	CAMK1D	FIG4	NAALADL2	SMIM13	
FMN2	CAPN9	FMN1	NAV2	SNORD113–2	
FTO	CAPZA1	FNDC3B	NAV3	SNRPD3	
FUS	CASC10	FRMD3	NCKAP5	SNTG2	
GLI2	CAST	GABBR2	NEIL3	SORBS2	
HIATL1	CCDC3	GALNT2	NELL1	SORCS2	
IL18RAP	CCDC81	GALNTL6	NFIA	SOX5	
IQGAP2	CD1A	GAS6	NLRP7	SOX7	
KALRN	CD1B	GCH1	NOTCH4	SPAG16	
KCNS3	CD1E	GFPT1	NOX4	SPATA13	
KIFAP3	CDH12	GFRA1	NPR3	SPG11	
KRT18P55	CDH23	GLIS3	NPTXR	SPTLC3	
LARGE	CDH4	GLT8D2	NRXN1	SRGAP3	
LOXHD1	CDH8	GMDS	NRXN3	SRRM4	
LRPPRC	CDK14	GNG7	NUDT12	STAC	
MAGI2	CDRT4	GNPDA1	NXPH1	STK36	
NEFH	CELF2	GPC6	OPTN	STX7	
NHSL1	CELF4	GPR176	ORC5	SUN3	
NKAIN2	CELSR1	GRB14	OSBP2	SYN3	
NSMAF	CEP44	GRIK2	OTP	SYNJ2	
OPCML	CGNL1	GRIK4	PA2G4P4	SYT9	
PCDH15	CHAF1A	GRIN2B	PACRG	SYTL3	
PCSK6	CHAMP1	GRM3	PALLD	TACR2	
PDE4B	CHGB	GRM7	PARK2	TANGO6	
PLXDC2	CHRM5	GRM8	PARVB	TANK	
PON2	CHST1	GRN	PASD1	TCEA1	
PTPRN2	CNTN3	HABP2	PAX7	TCF7L1	
PTPRT	CNTN4	HCFC2P1	PBX1	TCL1B	
RGS6	COL14A1	HDAC4	PCDH12	TIAM2	
ROBO2	COL1A1	HFE	PDCL3P1	TMEM132C	
SLC25A26	COL27A1	HHAT	PDE7B	TMEM135	
SNX29	COL28A1	HLA-DOA	PDZD2	TMEM91	
SPATA22	COLGALT2	HLA-DPB2	PEPD	TMPRSS13	
SPTLC1P2	CREB3L2	HLA-DRB9	PFKP	TMTC1	
SUSD1	CREB5	HMCN2	PHC1	TNPO3	
THSD7A	CRHBP	HNF1B	PIGL	TP63	

Table 9 (*continued*)

Gene name				
TIAM1	CRYGGP	HNRNPA1P32	PLA2G12B	TRAK2
TLR1	CSRP1	HPGD	PLCB1	TUFT1
TLR10	CST5	HS3ST4	PLEKHM3	TULP4
TMEM132D	CTNNA3	HSCB	PLGRKT	TXNRD1
TMEM163	CTNND2	HUS1	PON1	UBQLN2
TMTC2	CTSC	IFI44L	PPP1R14C	VAPB
UNC13C	CX3CR1	IFT74	PPP2R5E	VRK2
UPF2	CXCL12	IL1A	PRDM16	VSNL1
VEGFA	DAO	IL20RA	PRKAG2	WBSCR17
ZFP64	DBF4B	INSIG2	PRKCA	WDFY3
ACOXL	DCC	INSR	PRKCQ	WNT9A
ADAMTS20	DCLK1	IQCJ-SCHIP1	PRPH	WWOX
ADARB2	DCTN1	JARID2	PRR9	XRCC1
ADCY1	DGKB	KCNIP1	PSD3	YPEL1
ADH7	DIAPH3	KCNMA1	PTPRD	ZBTB20
ADRBK2	DIRC3	KCNMB3	PXDNL	ZFP36L1
AFTPH	DISC1	KCNN2	RAB3C	ZFPM2

Sources of Funding

This research was funded by Oxford BioDynamics as well as Innovate UK. Work in the Oxford Motor Neurone Disease Care and Research Centre is supported by grants from the Motor Neurone Disease Association and the Medical Research Council. MRT is funded by the Medical Research Council & Motor Neurone Disease Association Lady Edith Wolfson Senior Clinical Fellowship (MR/K01014X/1).

Author Contributions

The study was conceived and designed by M. Cudkowicz, J. Berry, E. Hunter and A. Akoulitchev. The manuscript was prepared by M. Salter (main author matthew.salter@oxfordbiodynamics.com), J. Green, J. Westra, A. Akoulitchev, M. Cudkowicz, L. Ossher and K. Talbot. Methodology development and data acquisition was done by M. Salter, J. Green, E. Corfield, L. Ossher and K. Talbot. Analysis and data interpretation were done by M. Salter, J. Green, J. Westra, E. Hunter, A. Ramadass, A. Akoulitchev and F. Grand.

Declaration of Interests

All authors (1) are employees of Oxford BioDynamics and are shareholders within the company. A. Akoulitchev and A. Ramadass are company directors. Oxford BioDynamics holds patents on the *EpiSwitch*™ technology. Authors (2) are employees of the University of Oxford, Nuffield Department of Clinical Sciences and Authors (3) is from Massachusetts General Hospital, Amyotrophic Lateral Sclerosis clinic and the Neurological Clinical Research Institute.

References

[1] Mitchell JD, Callagher P, Gardham J, Mitchell C, Dixon M, Addison-Jones R, et al. Timelines in the diagnostic evaluation of people with suspected amyotrophic lateral sclerosis (ALS)/motor neuron disease (MND) – a 20-year review: can we do better? Amyotroph Lateral Scler 2010;11:537–41. https://doi.org/10.3109/17482968.2010.495158.

[2] Chen S, Sayana P, Zhang X, Le W. Genetics of amyotrophic lateral sclerosis: an update. Mol Neurodegener 2013;8:28. https://doi.org/10.1186/1750-1326-8-28.

[3] Johnson JO, Mandrioli J, Benatar M, Abramzon Y, Van Deerlin VM, Trojanowski JQ, et al. Exome sequencing reveals VCP mutations as a cause of familial ALS. Neuron 2010;68:857–64. https://doi.org/10.1016/j.neuron.2010.11.036.

[4] Heyn H, Esteller M. DNA methylation profiling in the clinic: applications and challenges. Nat Rev Genet 2012;13:679–92. https://doi.org/10.1038/nrg3270.

[5] Qureshi IA, Mehler MF. Understanding neurological disease mechanisms in the era of epigenetics. JAMA Neurol 2013;70:703–10. https://doi.org/10.1001/jamaneurol.2013.1443.

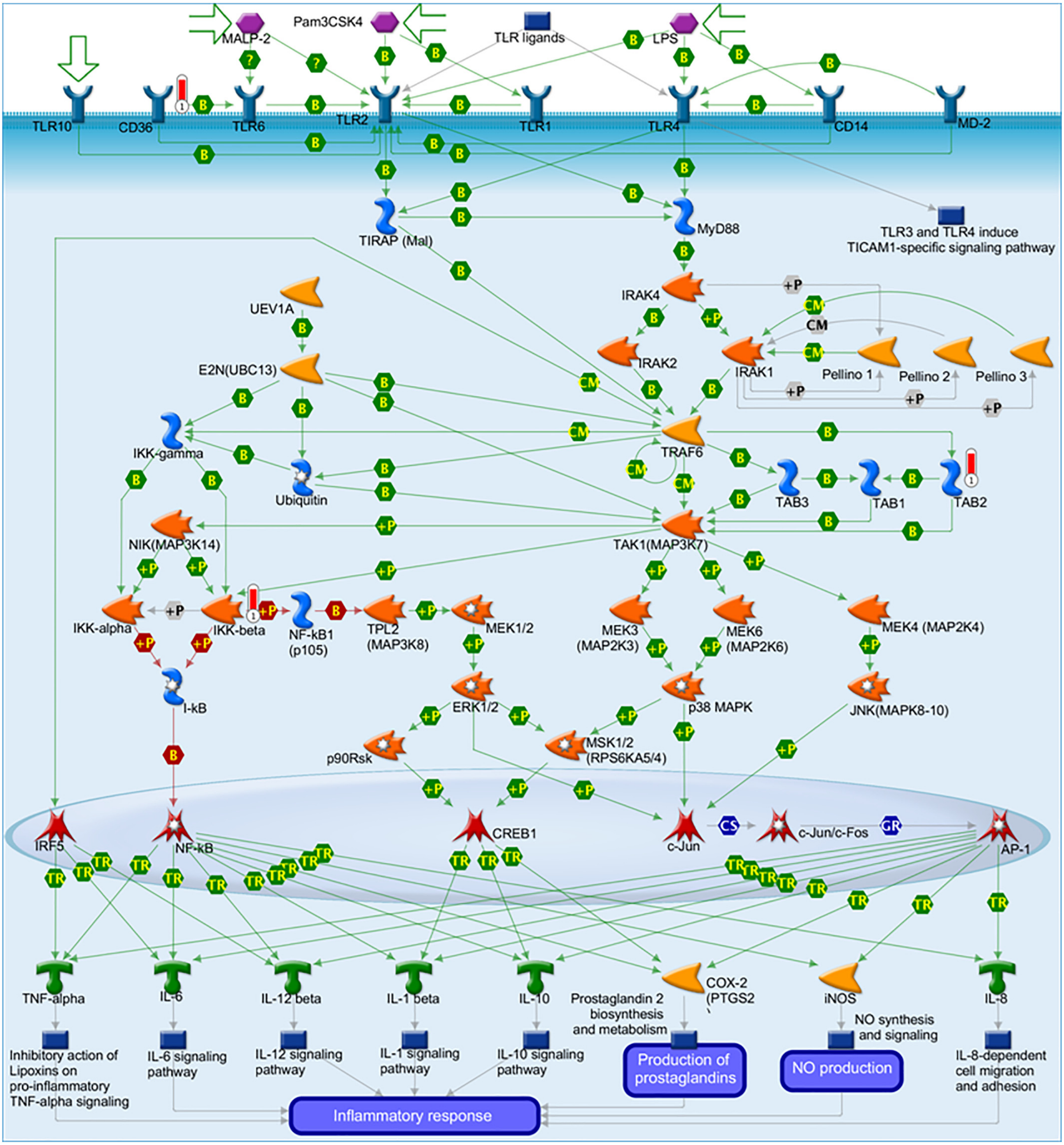

Fig. 3. Toll-like receptor signaling cascade showing the biological involvement of three of the eight chromosome conformation signature loci; CD36, TAB2 and IKKB (red thermometers) in the regulation of the inflammatory response. Image generated using Metacore™.

[6] Hunter E, Ramadass A, Womersley H, Akoulitchev A. Epigenetic footprints for neurodegenerative and autoimmune conditions: a comparative analysis. The Lancet Neurology Conference; 2016.

[7] Sherman A, Bowser R, Grasso D, Power B, Milligan C, Jaffa M, et al. Proposed BioRepository platform solution for the ALS research community. Amyotroph Lateral Scler 2011;12:11–6. https://doi.org/10.3109/17482968.2010.539233.

[8] Bastonini E, Jeznach M, Field M, Juszczyk K, Corfield E, Dezfouli M, et al. Chromatin barcodes as biomarkers for melanoma. Pigment Cell Melanoma Res 2014;27:788–800. https://doi.org/10.1111/pcmr.12258.

[9] Carini C, Hunter E, Ramadass AS, Green J, Akoulitchev A, Mcinnes IB, et al. Chromosome conformation signatures define predictive markers of inadequate response to methotrexate in early rheumatoid arthritis. J Transl Med 2018. https://doi.org/10.1186/s12967-018-1387-9.

[10] Jakub JW, Grotz TE, Jordan P, Hunter E, Pittelkow M, Ramadass A, et al. A pilot study of chromosomal aberrations and epigenetic changes in peripheral blood samples to identify patients with melanoma. Melanoma Res 2015. https://doi.org/10.1097/CMR.0000000000000182.

[11] McCord R, Sandmann T, Field M, Jordan P, Hunter E, Akoulitchev A, et al. Chromatin signatures of DLBCL subtypes. ACR Annual Meeting; 2014.

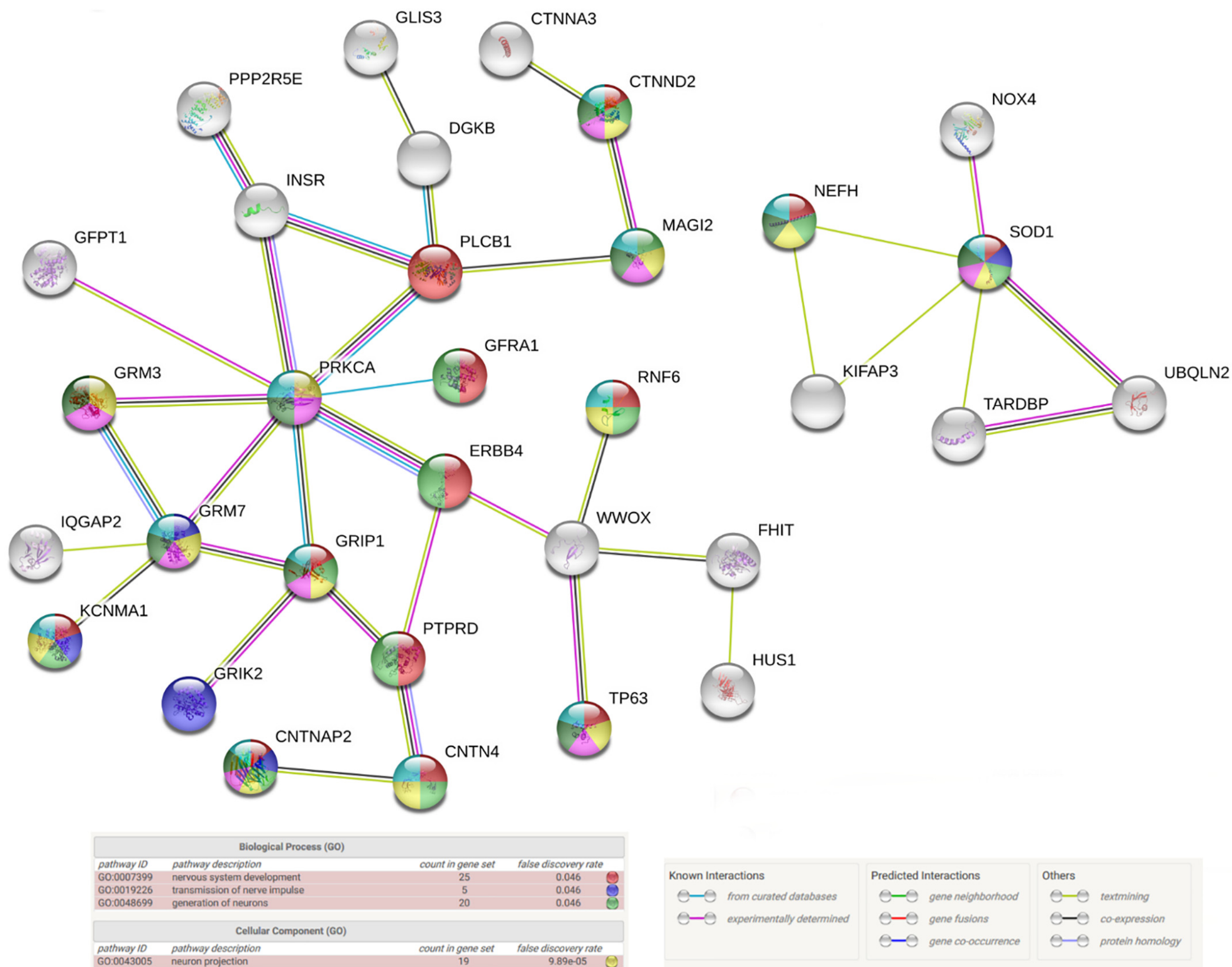

Biological Process (GO)			
pathway ID	pathway description	count in gene set	false discovery rate
GO:0007399	nervous system development	25	0.046
GO:0019226	transmission of nerve impulse	5	0.046
GO:0048699	generation of neurons	20	0.046

Cellular Component (GO)			
pathway ID	pathway description	count in gene set	false discovery rate
GO:0043005	neuron projection	19	9.89e-05
GO:0030425	dendrite	12	0.00163
GO:0036477	somatodendritic compartment	14	0.00163
GO:0097458	neuron part	18	0.00407

Fig. 4. Protein STRING network of ALS regulation. The gene loci for the top 150 chromosome conformations that could best discriminate between ALS samples and healthy controls in the second array screen were uploaded as proteins to the STRING database and a resulting interaction network was generated. The two main networks are shown. Network nodes represent proteins and edges represent protein-protein associations. All nodes shown are query proteins and the first shell of interactors. Nodes are colored according to their association with the top gene ontology (GO) terms for Biological Process and Cellular Component. Edges are colored according to their interactions, either known, predicted or other.

[12] Salter M, Elvidge W, Ramadass A, Womersley H, Grand F, Green J, et al. Epigenetic signatures and early detection of neurodegenerative diseases. The Lancet Neurology Conference. The Lancet Neurology Conference; 2016.

[13] Sangurdekar D, Plavina T, Singh C, Innis B, Enayetallah A, Subramanyam M, et al. Chromosome conformation capture to discover candidate epigenetic markers of multiple sclerosis disease severity. 32nd Congress of the European Committee for Treatment and Research in Multiple Sclerosis; 2016.

[14] Crutchley JL, Wang XQD, Ferraiuolo M a, Dostie J. Chromatin conformation signatures: ideal human disease biomarkers? Biomark Med 2010;4:611–29. https://doi.org/10.2217/bmm.10.68.

[15] Chen X, Shang H-F. New developments and future opportunities in biomarkers for amyotrophic lateral sclerosis. Transl Neurodegener 2015;4:17. https://doi.org/10.1186/s40035-015-0040-2.

[16] Nguyen DKH, Thombre R, Wang J. Autophagy as a common pathway in amyotrophic lateral sclerosis. Neurosci Lett 2018. https://doi.org/10.1016/j.neulet.2018.04.006.

[17] Su XW, Broach JR, Connor JR, Gerhard GS, Simmons Z. Genetic heterogeneity of amyotrophic lateral sclerosis: implications for clinical practice and research. Muscle Nerve 2014;49:786–803. https://doi.org/10.1002/mus.24198.

[18] Vajda A, McLaughlin RL, Heverin M, Thorpe O, Abrahams S, Al-Chalabi A, et al. Genetic testing in ALS: a survey of current practices. Neurology 2017. https://doi.org/10.1212/WNL.0000000000003686.

[19] Lai C, Xie C, McCormack SG, Chiang H-C, Michalak MK, Lin X, et al. Amyotrophic lateral sclerosis 2-deficiency leads to neuronal degeneration in amyotrophic lateral sclerosis through altered AMPA receptor trafficking. J Neurosci 2006;26:11798–806. https://doi.org/10.1523/JNEUROSCI.2084-06.2006.

[20] Landers JE, Melki J, Meininger V, Glass JD, van den Berg LH, van Es MA, et al. Reduced expression of the kinesin-associated protein 3 (KIFAP3) gene increases survival in sporadic amyotrophic lateral sclerosis. Proc Natl Acad Sci U S A 2009;106:9004–9. https://doi.org/10.1073/pnas.0812937106.

[21] van Doormaal PTC, Ticozzi N, Gellera C, Ratti A, Taroni F, Chiò A, et al. Analysis of the KIFAP3 gene in amyotrophic lateral sclerosis: a multicenter survival study. Neurobiol Aging 2014;35. https://doi.org/10.1016/j.neurobiolaging.2014.04.014.

[22] Bakkar N, Boehringer A, Bowser R. Use of biomarkers in ALS drug development and clinical trials. Brain Res 2015. https://doi.org/10.1016/j.brainres.2014.10.031.

[23] Byrne S, Walsh C, Lynch C, Bede P, Elamin M, Kenna K, et al. Rate of familial amyotrophic lateral sclerosis: a systematic review and meta-analysis. J Neurol Neurosurg Psychiatry 2011;82:623–7. https://doi.org/10.1136/jnnp.2010.224501.

[24] Simon NG, Turner MR, Vucic S, Al-Chalabi A, Shefner J, Lomen-Hoerth C, et al. Quantifying disease progression in amyotrophic lateral sclerosis. Ann Neurol 2014. https://doi.org/10.1002/ana.24273.

[25] Traynor BJ, Zhang H, Shefner JM, Schoenfeld D, Cudkowicz ME. Functional outcome measures as clinical trial endpoints in ALS. Neurology 2004;63:1933–5. https://doi.org/10.1212/01.WNL.0000144345.49510.4E.

[26] Debray S, Race V, Crabbé V, Herdewyn S, Matthijs G, Goris A, et al. Frequency of C9Orf72 repeat expansions in amyotrophic lateral sclerosis: a Belgian cohort study. Neurobiol Aging 2013;34. https://doi.org/10.1016/j.neurobiolaging.2013.06.009.

[27] Renton AE, Majounie E, Waite A, Simón-Sánchez J, Rollinson S, Gibbs JR, et al. A hexanucleotide repeat expansion in C9ORF72 is the cause of chromosome 9p21-linked ALS-FTD. Neuron 2011;72:257–68. https://doi.org/10.1016/j.neuron.2011.09.010.

[28] Dejesus-Hernandez M, Mackenzie IR, Boeve BF, Boxer AL, Baker M, Rutherford NJ, et al. Expanded GGGGCC hexanucleotide repeat in noncoding region of C9ORF72 causes chromosome 9p-linked FTD and ALS. Neuron 2011;72:245–56. https://doi.org/10.1016/j.neuron.2011.09.011.
[29] Majounie E, Renton AE, Mok K, Dopper EGP, Waite A, Rollinson S, et al. Frequency of the C9orf72 hexanucleotide repeat expansion in patients with amyotrophic lateral sclerosis and frontotemporal dementia: a cross-sectional study. Lancet Neurol 2012;11:323–30. https://doi.org/10.1016/S1474-4422(12)70043-1.
[30] Brites D, Vaz AR. Microglia centered pathogenesis in ALS: insights in cell interconnectivity. Front Cell Neurosci 2014;8. https://doi.org/10.3389/fncel.2014.00117.
[31] Miyamoto Y, Tamano M, Torii T, Kawahara K, Nakamura K, Tanoue A, et al. Data supporting the role of Fyn in initiating myelination in the peripheral nervous system. Data Br 2016;7:1098–105. https://doi.org/10.1016/j.dib.2016.03.096.
[32] Mihalas AB, Meffert MK. IKK kinase assay for assessment of canonical NF-κB activation in neurons. Methods Mol Biol 2015;1280:61–74. https://doi.org/10.1007/978-1-4939-2422-6_5.
[33] Lee J, Hyeon SJ, Im H, Ryu H, Kim Y, Ryu H. Astrocytes and microglia as non-cell autonomous players in the pathogenesis of ALS. Exp Neurobiol 2016;25:233–40. https://doi.org/10.5607/en.2016.25.5.233.
[34] Berry JD, Taylor AA, Beaulieu D, Meng L, Bian A, Andrews J, et al. Improved stratification of ALS clinical trials using predicted survival. Ann Clin Transl Neurol 2018. https://doi.org/10.1002/acn3.550.
[35] Taylor AA, Fournier C, Polak M, Wang L, Zach N, Keymer M, et al. Predicting disease progression in amyotrophic lateral sclerosis. Ann Clin Transl Neurol 2016. https://doi.org/10.1002/acn3.348.
[36] Julien JP. Amyotrophic lateral sclerosis: unfolding the toxicity of the misfolded. Cell 2001. https://doi.org/10.1016/S0092-8674(01)00244-6.
[37] Bowerman M, Vincent T, Scamps F, Perrin FE, Camu W, Raoul C. Neuroimmunity dynamics and the development of therapeutic strategies for amyotrophic lateral sclerosis. Front Cell Neurosci 2013;7:214. https://doi.org/10.3389/fncel.2013.00214.
[38] Krieger C, Lanius RA, Pelech SL, Shaw CA. Amyotrophic lateral sclerosis: the involvement of intracellular Ca2+ and protein kinase C. Trends Pharmacol Sci 1996;17:114–20.
[39] Lanius RA, Paddon HB, Mezei M, Wagey R, Krieger C, Pelech SL, et al. A role for amplified protein kinase C activity in the pathogenesis of amyotrophic lateral sclerosis. J Neurochem 1995;65:927–30. https://doi.org/10.1046/j.1471-4159.1995.65020927.x.
[40] Battaglia G, Bruno V. Metabotropic glutamate receptor involvement in the pathophysiology of amyotrophic lateral sclerosis: new potential drug targets for therapeutic applications. Curr Opin Pharmacol 2018. https://doi.org/10.1016/j.coph.2018.02.007.
[41] Chiò A, Logroscino G, Traynor B, Collins J, Simeone J, White LA. Global epidemiology of amyotrophic lateral sclerosis (ALS): a systematic review of the literature. Amyotroph Lateral Scler 2012;13:126.
[42] Vu LT, Bowser R. Fluid-based biomarkers for amyotrophic lateral sclerosis. Neurotherapeutics 2017. https://doi.org/10.1007/s13311-016-0503-x.
[43] Marin B, Boumédiene F, Logroscino G, Couratier P, Babron M-C, Leutenegger AL, et al. Variation in worldwide incidence of amyotrophic lateral sclerosis: a meta-analyss. Int J Epidemiol 2016. https://doi.org/10.1093/ije/dyw061.
[44] Roberts AL, Johnson NJ, Chen JT, Cudkowicz ME, Weisskopf MG. Race/ethnicity, socioeconomic status, and ALS mortality in the United States. Neurology 2016;87:2300–8. https://doi.org/10.1212/WNL.0000000000003298.
[45] Feinberg AP. The key role of epigenetics in human disease prevention and mitigation. N Engl J Med 2018;378:1323–34. https://doi.org/10.1056/NEJMra1402513.
[46] Prattichizzo F, Micolucci L, Cricca M, De Carolis S, Mensà E, Ceriello A, et al. Exosome-based immunomodulation during aging: a nano-perspective on inflamm-aging. Mech Ageing Dev 2017. https://doi.org/10.1016/j.mad.2017.02.008.
[47] Ratajczak MZ, Ratajczak J. Horizontal transfer of RNA and proteins between cells by extracellular microvesicles: 14 years later. Clin Transl Med 2016. https://doi.org/10.1186/s40169-016-0087-4.
[48] Li DW, Liu M, Cui B, Fang J, Guan YZ, Ding Q, et al. The Awaji criteria increases the diagnostic sensitivity of the revised El Escorial criteria for amyotrophic lateral sclerosis diagnosis in a Chinese population. PLoS One 2017:12. https://doi.org/10.1371/journal.pone.0171522.
[49] Oeckl P, Jardel C, Salachas F, Lamari F, Andersen PM, Bowser R, et al. Multicenter validation of CSF neurofilaments as diagnostic biomarkers for ALS. Amyotroph Lateral Scler Front Degener 2016;17:404–13. https://doi.org/10.3109/21678421.2016.1167913.